

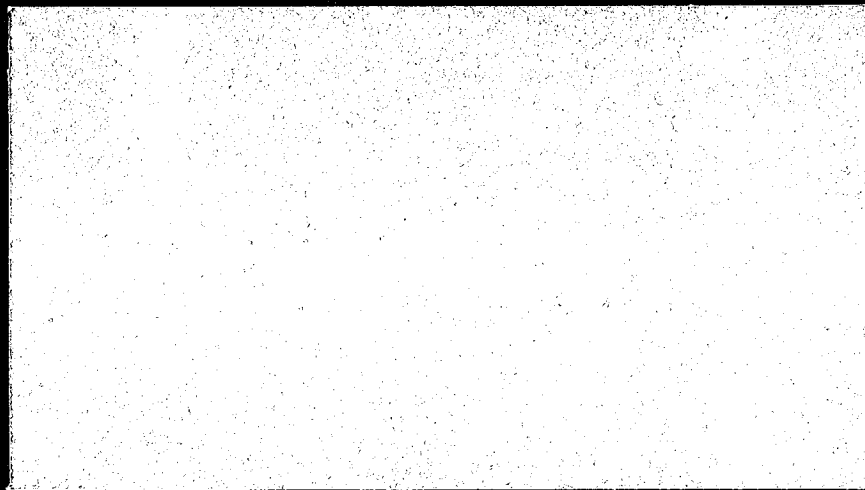
The George W. Woodruff School of Mechanical Engineering

(NASA-CR-182583) AN OPPOSED-BUCKET LUNAR
DIGGING IMPLEMENT Advanced Missions Space
Design Program (Georgia Inst. of Tech.)
120 p

N90-71235

Unclass

00/37 0280006



Georgia Institute of Technology

Atlanta, Georgia 30332



GEORGIA TECH 1885-1985

DESIGNING TOMORROW TODAY

THE GEORGE W. WOODRUFF SCHOOL OF
MECHANICAL ENGINEERING

ME 4182
MECHANICAL DESIGN ENGINEERING

NASA/UNIVERSITY
ADVANCED MISSIONS SPACE DESIGN PROGRAM

AN OPPOSED-BUCKET LUNAR DIGGING IMPLEMENT

JUNE 1987

ORIGINAL CONTAINS
COLOR ILLUSTRATIONS

Marshall B. Allen, III
Chih-Yu Chu
Jon M. Coleman
Jae N. Lim
Paul R. Thomas
Bertram B. Wheatley

Georgia Institute of Technology
Atlanta, Georgia 30332-0405

LUNAR DIGGER

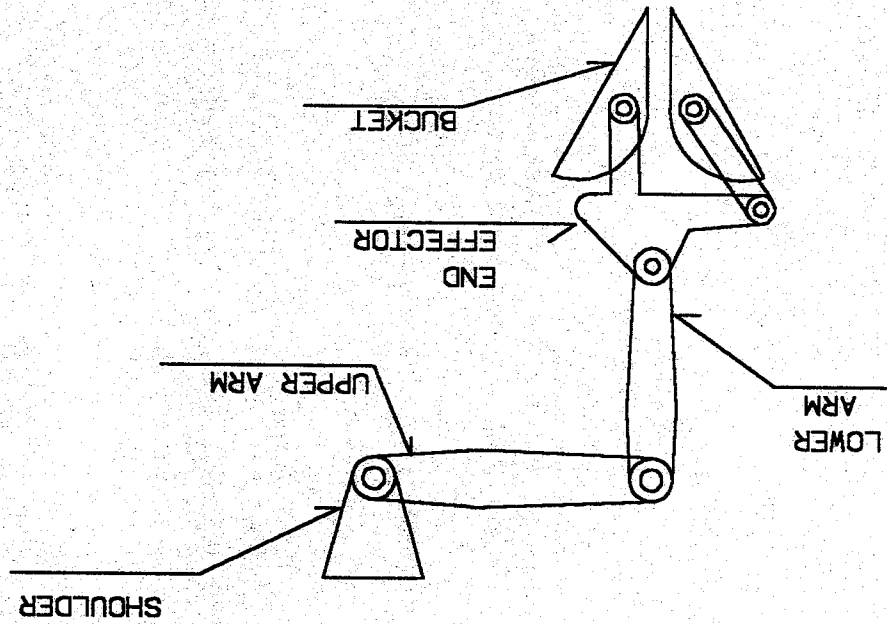


TABLE OF CONTENTS

I. Abstract.....	ii
II. Problem Statement.....	1
A. Constraints.....	2
B. Environments.....	2
C. Weight.....	3
D. Focus and Organization.....	4
III. Description of Operation.....	5
IV. Performance.....	6
V. Dimensions of Upper and Lower Arm.....	7
VI. Hydraulic System.....	8
VII. Heat Transfer and Thermal Control.....	10
VIII. Interface Pin Connection and Joints.....	12
IX. Power Supply.....	16
X. Controls.....	17
XI. Weight.....	20
XII. Conclusion.....	21
XIII. Recommendation.....	22
XIV. Acknowledgements.....	23
XV. Bibliography.....	24
XVI. Appendices	
1. Structure.....	26
2. Power System Comparsion.....	42
3. Hydraulics.....	45
4. Heat Transfer.....	62
5. Performance.....	76
6. Interface Pin Connection.....	78
7. Joints.....	89
8. Progress Report.....	99

ABSTRACT

The Lunar Digger has been worked on by several groups this year. Many problems have been solved, but the digger is far from complete. The arm and shoulder need to be analyzed for the 20 KN pecking force, and lubrication options need to be stated. Electromechanical actuators were not researched in depth; therefore, a further comparison must be made to clarify the previous decision to use hydraulic actuators. In addition, heat transfer and control systems must be designed since past reports left out these important subjects.

Information on heat transfer, controls, lubrication, electromechanics, and hydraulics were researched through textbooks and professors. A force analysis on the arm and shoulder was made to check the material, and programs on heat dissipation were used to design an acceptable heat transfer system.

Results indicate that the kinematic structure should use a 1.3 meter pecking distance, a Teflon coating, a hydraulic power system, a radiator heat transfer device, and a simple closed loop feedback control system. We conclude that the corrective actions and additions should be made in order to further optimize the design.

PROBLEM STATEMENT

In recent years the long term planning decision of the National Aeronautics and Space Administration, NASA, has proposed the construction of bases on the Moon for the purpose of lunar research and exploration. To accomplish such a project, construction vehicles equivalent to bulldozers and earthmovers on earth must be designed for the moon. Of particular importance is a lunar digging mechanism which is imperative for the excavation of the lunar surface in order to lay the foundations for such a base. The preliminary design for such a digging mechanism, or a Lunar Digger, has been accomplished by previous project groups. The purpose of our project group is to further develop the Lunar Digger to a final optimized design. The digger's objectives include impacting the soil for penetration, trenching, rock removal, and surface leveling. The word "lunar" simply describes something that pertains to the moon, while the word "digger" is self-explanatory.

To achieve our purpose, we must specify a power generation and transmission system, a heat transfer system, a lubrication scheme, a control system, and an improved kinematic structure. The performance levels that need to be achieved include a day and

night operational machine, a life expectancy of ten years for the arm structure itself, a damping of the 20KN pecking impact force, and an operational control format.

CONSTRAINTS

The moon's environment and the weight of the digging implement are the main constraints in the design of the lunar digger. Both constraints must be taken into consideration for an efficient working model.

ENVIRONMENTAL

Temperature gradient, lack of atmosphere, reduced gravity, radiation, and soil mechanics are the major environmental constraints of the moon. Since the diggers on the earth are not suited for the moon, information gained from experience with earth vehicles is limited.

The temperature gradient of materials on the Moon is steep. In the shade, the temperature will be at -130 degrees C. On the other hand, in the sunlight, the temperature is at +100 degrees C. Materials used for the digger must function in this wide range of temperatures. Hydraulic fluids, power systems, and controls are also subject to the extreme temperature gradient.

The atmosphere of the moon is one-two millionth that of the

earth. The assumption that the atmosphere is virtually non-existent can be readily made. One resulting constraint is that there is no medium to transfer heat by conduction or convection. Therefore, the motor and the material will have to use an alternative method in transferring heat. The joints of the members are also subjected to cold welding if metal to metal contact is made. Lubrication that can withstand the lack of atmosphere and abrasion are vital for the joints.

Radiation has one major effect on the design of the model. The ultraviolet radiation that reaches the implement will deteriorate any non-metallic substances. Rubber seals would deteriorate and cause breakdown if the seals were used on the digger. Radiation would also have the same effect on the protective covering.

The soil on the moon is very abrasive. Lunar dust and soil will wear down metal and tear seals. The surface may have rocks and hard crusts that resemble gravel on the earth. The digger must operate under these conditions and still remove the soil and rock as well. Joints and outer surface must be protected, and the scoops should have a high resistance to wear.

WEIGHT

The weight constraint of 6700 N is used to restrict the

costs of transporting the materials. The estimated cost for transporting materials to the moon is \$3,400 per N.

FOCUS AND ORGANIZATION

The Lunar Digger is a complex mechanical machine composed of many systems. This report details the improvements and optimizations made in the design of the arm and shoulder structure, the lubrication system, the power system, the heat transfer system, and the control system. The details concerning the analysis and design of each of the above systems are organized in individual sections that will follow.

DESCRIPTION OF OPERATION

The Lunar Digger is very similar in appearance to a backhoe. However, constraints of the lunar environment dictate that the digger will differ significantly in operation.

An earth bound backhoe uses its weight and the weight of the significantly massive attached equipment to provide the re-action forces necessary to insert the bucket into the soil.

First, the bucket is inserted into the soil using the weight for a normal force reaction, penetrating the soil. After penetration, a lateral force is added and draws the bucket not only downward, but horizontally through the soil, filling the bucket. This is an efficient method of digging on earth, but on the lunar surface, the decrease in gravity to $1/6$, or 17% of the earth's gravity poses problems. The same mass on the moon simply will not provide enough weight form the reaction forces necessary to penetrate the lunar crust.

The Lunar Digger has available to it approximately 1,350N normal force and 140N lateral force available for digging (from the combined weight of the Skitter and Digger). To circumvent the lack of stationary reaction force, the digger arm and the end-effector buckets will be accelerated downward before impacting the surface.

The momentum gained will then be the used to initially insert the bucket tips into the lunar soil. The opposed bucket design effectively pulls itself into the soil to complete the digging cycle.

PERFORMANCE

There could be times when it would be helpful to know the digging rate of the digger. This rate was calculated in appendix (V) and was found to be 260 cubic meters per hour.

DIMENSIONS OF THE UPPER AND LOWER ARM

The dimensions of the arms are determined from the impact force of 25 KN on the hydraulics. Free body diagrams and a program determining inertia and stress show the regions of safety for the members. The yeild strength of 390 MN/m² and a factor of safety of 2 give the admissible stress from bending to be 180 MN/m². We chose the stress of 147 MN/m² to assure buckling does not occur across the secondary axis. The buckling calculations are made at the cross-section where the hydraulics are located. The dimensions of the arms can be shown in tabular form. Calculations and visuals of the arm are in Appendix 1. The total weight of the arms is 185 N (41lbs).

	<u>UPPER ARM</u>	<u>LOWER ARM</u>
L	1.94 m	1.5 m
H	.1-.16 m	.1-.14 m
B	.08 m	.07 m
t	.01 m	.01 m

L = LENGTH

H = HEIGHT

B = WIDTH

t = THICKNESS

(*NOTE: THE WIDTH AND HEIGHT TAPER FROM THE HIGH TO LOW STRESS)

HYDRAULIC SYSTEM

The Lunar Digger will be powered by a system of eight hydraulic actuators. There will be one rotary and seven linear actuators as shown in figure (III-1). A list of these actuators can be found in table (III-2).

	Bore	Rod	Minimum	Maximum	
Label:	Diameter:	Diameter:	Length:	Length:	Power:
	(cm)	(cm)	(m)	(m)	(kw)
2	2.5	1.3	.3	1.1	2
3	2.5	1.3	.3	1.1	2
4	5	2.5	1.5	3	10
5	2.5	1.3	.8	1.5	2
6	2.5	1.3	.5	1	2
7	3.8	1.9	.8	1.5	4
8	3.8	1.9	.8	1.5	4

Table III-2. Linear actuators.

The rotary actuator will rotate the digger about the shoulder pin at a speed of 7.5 rev/min. It must deliver a torque of 15,000 Nm and use 20 kw of power. These dimensions were obtained using an analysis of the envelope of the digger, force analysis on the digger and the force equations found in appendix (III). The digger will require 200 cubic centimeters of hydraulic fluid. The estimation of weight for the hydraulic system is 1500 N. This includes actuators, pump, hoses, connections and fluid.

HEAT TRANSFER AND THERMAL CONTROL

The space radiator panel consists of an aluminum panel with foam backing and a piping system machined into it. The panel is 1 meter high, 1 meter wide, and 0.1 meters thick. (See Figure 4.6.) A connector is welded into the entrance and exit of the panel to accomodate connection to hydraulic lines. The required panel size needed to cool the arms alone is sufficiently small to warrant the use of the hydraulic fluid to cool the entire structure. The hydraulic fluid will be shut off from the space radiator during cold hours to maintain a temperature between 477 Kelvin and 219 Kelvin. The only heat input during cold periods will come from running the electric motor and the hydraulic pump. Temperature loss in the fluid flowing in the pipes during cold hours can reach temperatures below acceptable levels if the arms are not insulated from the cold. (See Figure 4.2.)

Two slider crank mechanisms will be used to position the panel away from the digger arm. Each arm will be 0.1m x 0.1m. The crank arm is 0.5 meters long and the follower arm is 1.25 meters long. An HP cantilever beam program was used to size these linkages. The follower arm will have a brace at its end that will hold the arms together in their fully extended position. The arms have been designed to take the full load of the space radiator panel, 443 N, and are placed slightly below the panel's center of gravity, 0.01 meters, in order to lean the panel slightly towards the ground without the influence of the steel wire. A steel wire attached to an electric motor will be attached to the top middle

of the space radiator panel in order to tilt the panel in any desired direction and to lift the panel in order to start retracting the panel. This design can be extended and retracted manually under the condition that the motor fails.

In analyzing the heat transfer, the following assumptions were made: temperature of the hydraulic fluid is 470 K; panel is heated to 470 K; 85% efficient hydraulic pump; 822 watts of heat from the electric motor; emissivity = 0.8; absorptivity = 0.2; temperature of deep space = 210 K; arms are coated to achieve the stated emissivity and absorptivity of the space radiator; and 470 K accounts for all heat inputs into the fluid.

INTERFACE PIN CONNECTION

The digger was designed so that it can be attached to the under side of Skitter--the tripod construction base of the lunar arthropod walker. The connection between the digger and skitter is achieved by an interlocking pin mechanism. Three pins will be welded to the digger. The diameter of the interconnecting pin is 15 mm. Titanium alloy (ASTM), Grade 5 with tensile strength of 900 Mpa and a yield strength of 830 Mpa was chosen for our design material. This choice is the best because it has high strength, low cost, low density, good mechanical properties, and low coefficient of thermal expansion compared to other metal alloys, which are all desirable in our design.

The actual dimensions were obtained using the following equations and figure 6-1.

$$S_e = K_a K_b K_c K_d K_e S'_e \quad (1)$$

$$\sigma_a \leq S_a / 3 \quad (2)$$

The result from equation (1) using geometric stress-concentration factor of 4 with $D/d=2$ and $r/d=1.5$, infinite life, ground finished, 95% reliability, and safety factor of 3 is 82 Mpa. (See

appendix 6.) The diameter of the connecting pin was found to be greater than or equal to 15mm using equation (2) and figure 6-1, and results from equation (1). We therefore chose 15mm diameter for the connecting pin.

JOINTS

Pins

The joints of the digger mechanism are pin joints. Force analysis are done on the members to find the maximum loads that are imposed upon the joints. The pin sizes are then specified with the ability to withstand these maximum shear loads which are 25 kN for impact loading, and .55 kN for static loading. An example of this calculation is shown in appendix 7.

The .55 cm radius pins made out of 13V-11Cr-3Al Titanium Alloy are used at the connections between the shoulder and the upper arm, at the elbow of the upper and lower arms, and also at the connection of the lower arm and the end effector. A .96 cm radius pin made of the same Titanium Alloy is adopted for the use of connecting the hydraulic actuators to the frame of the digger.

Bearings

The Fiberglide self-lubricating bearings cited by last quarter's report seems to be a good choice for the moon's environment. With its load-carrying capacity listed up to 69,000 kN per square meter, it more than satisfies our requirement of 9,000 kN per square meter on the pin. (See Appendix 7). It also has a low coefficient of friction and high wear resistance which

will help in extending the life of the pins compare to use of normal bearings.

The CJS and LTD type bearings are used in our design in the following method: By cutting a key-slot for the pin and the casing of the outside arm, when a key is inserted, the pin will be rigid with the outer arm. On the other arm, a CJS type bearing is inserted to the arm's pin hole, this will allow the arm to rotate about the pin with ease. Two LTD type bearings are incorporated in the joints so that the arm will not have contact with each other. (See Figure 7-2).

POWER SUPPLY

The power source will be hydrogen/oxygen fuel cells. One important characteristic of the fuel cell is that, unlike batteries, fuel cells can be refilled by resupplying the fuel and oxidant sources. The fuel cells can also be constructed modularly for ease of service or replacement.

The fuel cells of the Space Shuttle Orbiters were used as a design guide since they are the most recent models actually tested. With an energy density of .15 kW/kg, the digger fuel cells will have a mass of 90 kg. It will have dimensions of 35 cm high x 38 cm wide x 100 cm long. The power supply is 7 kW average load, and 12 kW peak load. Fuel consumption is 50 kg of H₂ and O₂ each 24 hour day. It can be serviced every 3 days and has service ceiling of 2000 hours.

CONTROLS

The control system is primarily concerned with the motion of the linear actuators. Velocity, displacement, and external noise are fed back by a closed-loop, feedback system controlled by a computer. (See Figure 4.) There will be one rotary actuator as well.

A basic outline for the rotary control system can be explained below. The single chip microcomputer is used to analyze the input/output loop. To feedback the output, a tachometer measures the speed, and a position sensor measures the displacement. The potentiometer is used to find the position by the different voltages induced by the variable resistor.

The measurement of the linear motion can be achieved by alternative devices. Previously, the tachometer is used to measure the rotary motion. However, gears that convert linear to rotary motion may freeze, eliminating the possibility of using the tachometer for linear actuators. A LVDT can measure displacement with an accuracy of .01%, but the LVDT will not last or work on the moon. The solution to this problem can be solved by measuring the flow rate into the hydraulic cylinders. By dividing the flow rate of the hydraulic fluid by the cross-sectional area, the velocity of the actuator can be obtained. A set flow rate can also be calculated to determine the speed needed. Using numerical methods to integrate the flow rate will give the volume of the fluid in the cylinders. Dividing this volume by the cross-sectional area will give the position.

Joint PID Control

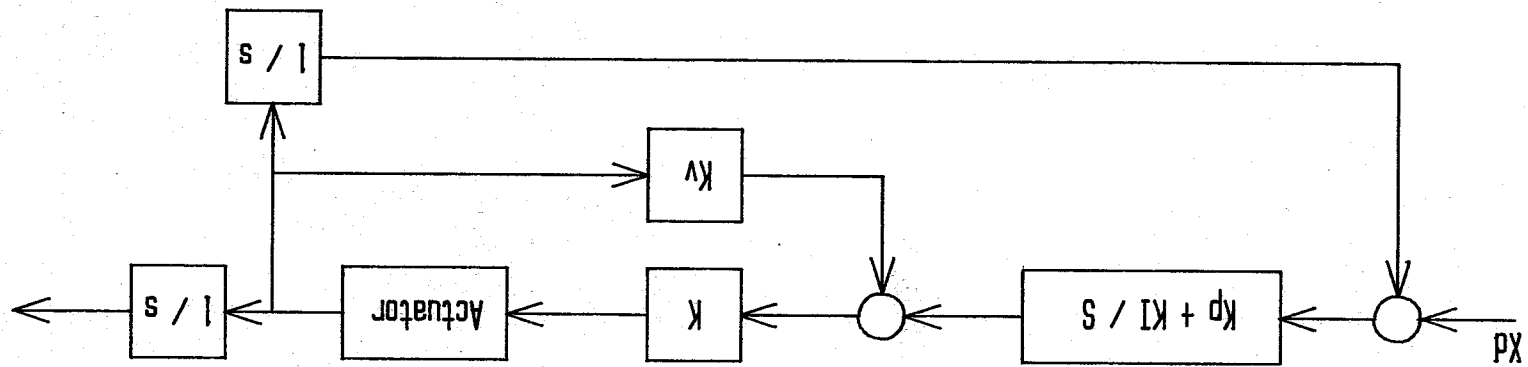
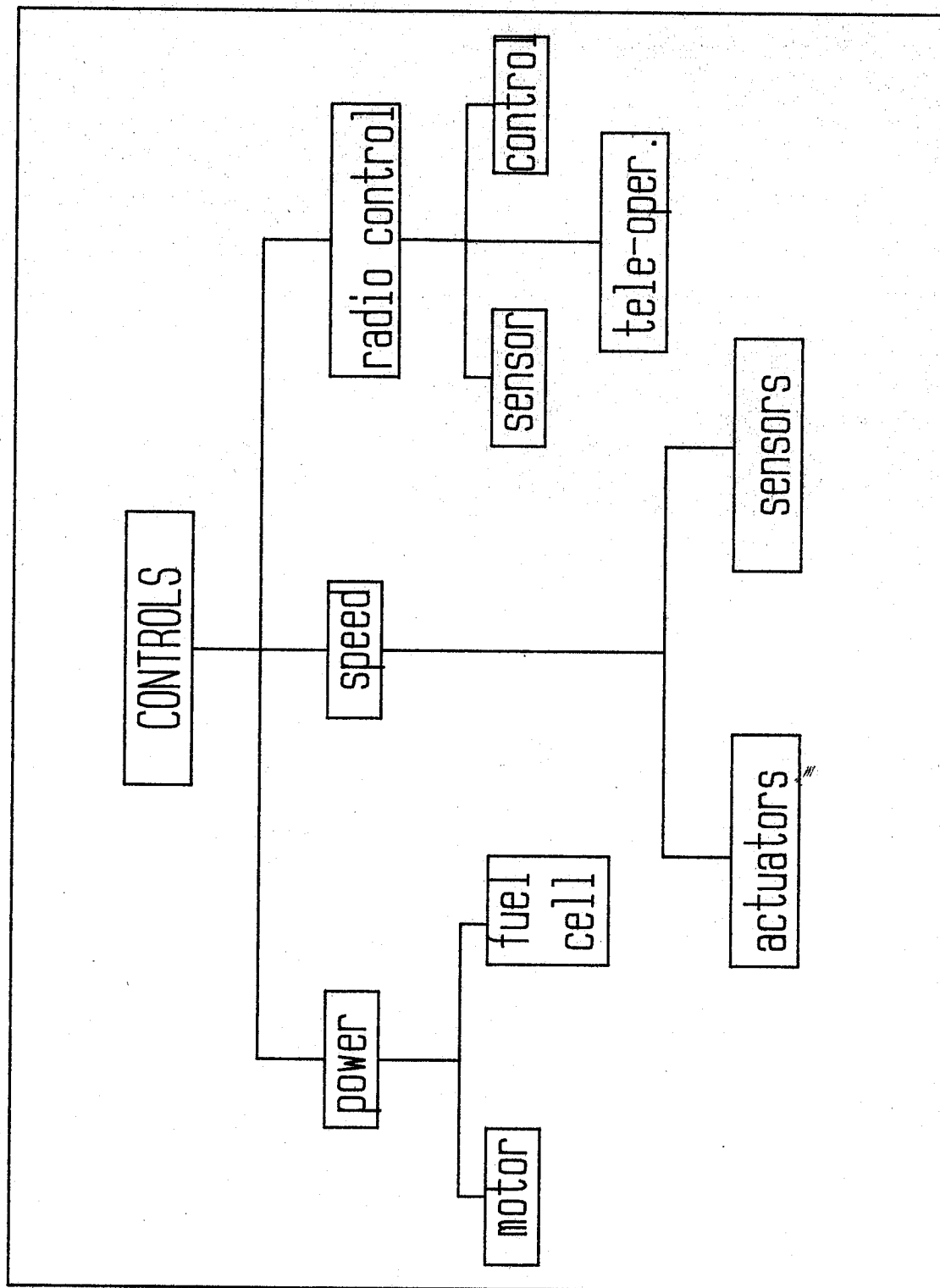


FIGURE 4



WEIGHT

The total weight of the system taken from each previous section is listed below. The weights are in earth newtons.

HYDRAULICS -	1500 N
END EFFECTOR -	1400 N
2 BUCKETS -	1100 N
FUEL CELL -	900 N
INTERFACE PLATE -	710 N
RADIATOR -	440 N
UPPER AND LOWER ARMS -	185 N
MOTOR -	75 N
SHOULDER -	70 N
<u>MISCELLANEOUS -</u>	<u>450 N</u>

TOTAL ESTIMATED WEIGHT - 6800 N (1500 LBS)

NOTE: THE MISCELLANEOUS WEIGHT INCLUDES SUCH OBJECTS AS INSULATION, CONTROLS, WIRING, PINS, AND JOINTS.

CONCLUSION

The performance objectives of the Lunar Digger have been closely met in this report. The required fuel cell, motor, joints, and interface pin connection are specified. The design of the radiator shows promise in transferring heat, but problems in the freezing of the fluid still exist. Although previous reports analyzed the hydraulic system and structure of the Lunar Digger, we still made improvements in the design. Examples of improvements would be the structures stronger resistance to torsion or moments about the secondary axis, and the force analysis on the hydraulic system during pecking.

The lack of analysis of the heat transfer system was a primary flaw in previous reports, so our design of a heat exchanger is immediately an improvement on the Lunar Digger Design. The end effector was the primary focus of last quarter's design group, so we accepted their recommendations and tried to improve from there. No weight or speed in digging improvement is obtained from this report, but efficient power systems are specified.

RECOMMENDATIONS

The Lunar Digger group of this quarter recommend that the Lunar Digger project be made more specific in detail. The project now seems to require a repetition of research and analysis. Topics such as the radiator and the control system would provide plenty of work for one quarter. Our group did not do an in depth control analysis, since we felt the need to repeat all the analysis of previous reports, with the exception of the end-effector.

There still exists flaws in the radiator and hydraulic design. So further research must be done in these areas. The Lunar Digger is by no means ready for the moon, although the design is capable of withstanding the moon's environment.

ACKNOWLEDGEMENTS

The authors of this report would like to express their warm gratitude to Mr. Jim Brazell for his support and encouragement in making this report possible. In addition, the authors would like to thank Drs. Sam Shelton and Gene Calwell for their assistance in providing technical information concerning the usage of heat pumps and space radiator on the moon.

BIBLIOGRAPHY

Budinski, kenneth. Engineering Materials, properties and selection 2nd ed. Reston, Virginia: Reston Publishing Co. Inc., 1983.

Calwell, Gene. Personal interview on Georgia Institute of Technology campus, Atlanta, Georgia. May 1987.

Last quarter's project. Digger and Bucket Report.

Lienhard, John H. Heat Transfer. Englewood Cliff: Prentice-Hall, Inc., 1981.

Mazzolani, F. M. Aluminum Alloy Structure. Institute of Construction Technology, University of Naples., Pitman Publishing Inc., 1985.

Sawyer, Kent. Design of a Samarium Cobalt Brushless DC Motor for Electromechanical Actuator Applications. Delco Electronics and J. T. Edge, NNSA Johnson Space Center, 1977.

Shelton, Samuel. Personal interview on Georgia Institute of Technology campus, Atlanta, Georgia. April 1987

Shigley, Joseph E. and LARRY D. Mitchell. Mechanical Engineering Design, Fourth Ed. New York: McGraw-Hill, Inc., 1983.

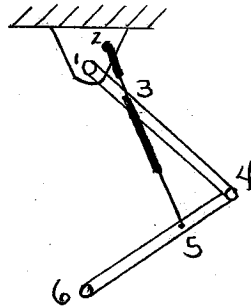
VSMF File. Fiberglide, Self-Lubricating Bearing, Lear Stegler
Inc.

Yeaple, Frank. Fluid Power and Control. New York: Marcel Dekker,
Inc., 1984.

APPENDIX 1

STRUCTURE

HYDRAULIC FORCE ANALYSIS

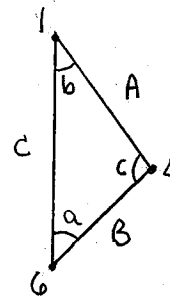


#1

$$C^2 = A^2 + B^2 - 2AB \cos(C)$$

A = 1.94, B = 1.5m ENTER C,

$$\sin(C)/C = \sin(B)/B = \sin(A)/A$$

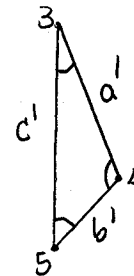


#2

$$C'^2 = A'^2 + B'^2 - 2A'B' \cos(C')$$

A' = 1.3 m, B' = .5 m

$$\sin(C')/C' = \sin(B')/B' = \sin(A')/A'$$



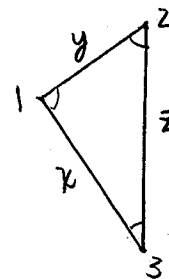
#3

$$Z^2 = Y^2 + X^2 - 2YX \cos(Z)$$

ANGLE Z = (180-36.87)-ANGLE B DEGREES

X = .7 m, Y = .5 m

$$\sin(Z)/Z = \sin(Y)/Y = \sin(X)/X$$



W

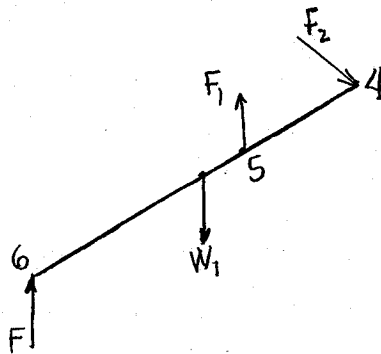
LOWER_ARM

BY SUMMING THE MOMENTS

$$F_1 = (F \cdot \sin(A) \cdot B - W_1 \cdot \sin(A) \cdot B/2) / \sin(A') \cdot B'$$

$$F_2 = (F \cdot \sin(A) \cdot (B - B') - W_1 \cdot \sin(A) \cdot (B/2 - B')) / B' \cdot \sin(C)$$

W1 = WEIGHT OF UPPER ARM



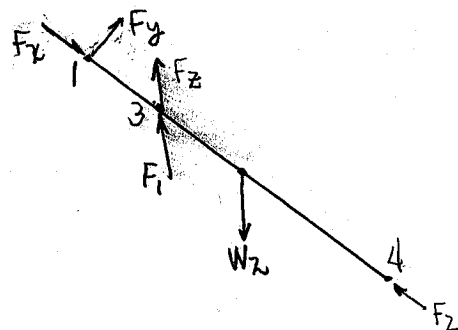
UPPER_ARM

$$F_Z = (W_2 \cdot \sin(B) \cdot A/2 - F_1 \cdot \sin(B') \cdot X) / X \cdot \sin(Y)$$

$$F_Y = 0$$

$$F_X = -(F_1 \cdot \cos(B') + F_Z \cdot \cos(Y)) + W_2 \cdot \cos(B) + F_2$$

W2 = WEIGHT OF UPPER ARM



x1 (m)	Mab (Nm)	x2 (m)	Mbc (Nm)	ARM HEIGHT (h)	y/I
0.00E+00	0.00E+00	7.00E-01	1.12E+04	1.00E-01	3.49E+04
1.00E-01	1.60E+03	8.00E-01	1.03E+04	1.10E-01	2.84E+04
2.00E-01	3.20E+03	9.00E-01	9.38E+03	1.20E-01	2.36E+04
3.00E-01	4.79E+03	1.00E+00	8.48E+03	1.30E-01	1.99E+04
4.00E-01	6.39E+03	1.10E+00	7.58E+03	1.40E-01	1.70E+04
5.00E-01	7.99E+03	1.20E+00	6.68E+03	1.50E-01	1.47E+04
6.00E-01	9.59E+03	1.30E+00	5.77E+03	1.60E-01	1.29E+04
7.00E-01	1.12E+04	1.40E+00	4.87E+03	1.70E-01	1.13E+04
		1.50E+00	3.97E+03	1.80E-01	1.01E+04
		1.60E+00	3.07E+03	1.90E-01	9.00E+03
		1.70E+00	2.16E+03		
		1.80E+00	1.26E+03		
		1.90E+00	3.61E+02		

1.94E+00 0.00E+00

0.00E+00	1.00E-01	2.00E-01	3.00E-01	4.00E-01	5.00E-01
0.00E+00	5.58E+07	1.12E+08	1.67E+08	2.23E+08	2.79E+08
0.00E+00	4.54E+07	9.09E+07	1.36E+08	1.82E+08	2.27E+08
0.00E+00	3.78E+07	7.55E+07	1.13E+08	1.51E+08	1.89E+08
0.00E+00	3.19E+07	6.37E+07	9.56E+07	1.27E+08	1.59E+08
0.00E+00	2.72E+07	5.45E+07	8.17E+07	1.09E+08	1.36E+08
0.00E+00	2.36E+07	4.71E+07	7.07E+07	9.42E+07	1.18E+08
0.00E+00	2.06E+07	4.12E+07	6.17E+07	8.23E+07	1.03E+08
0.00E+00	1.81E+07	3.63E+07	5.44E+07	7.25E+07	9.06E+07
0.00E+00	1.61E+07	3.22E+07	4.83E+07	6.43E+07	8.04E+07
0.00E+00	1.44E+07	2.87E+07	4.31E+07	5.75E+07	7.19E+07

6.00E-01	7.00E-01	8.00E-01	9.00E-01	1.00E+00	1.10E+00
3.35E+08	3.90E+08	3.59E+08	3.27E+08	2.96E+08	2.64E+08
2.73E+08	3.18E+08	2.92E+08	2.67E+08	2.41E+08	2.16E+08
2.27E+08	2.64E+08	2.43E+08	2.22E+08	2.00E+08	1.79E+08
1.91E+08	2.23E+08	2.05E+08	1.87E+08	1.69E+08	1.51E+08
1.63E+08	1.91E+08	1.75E+08	1.60E+08	1.45E+08	1.29E+08
1.41E+08	1.65E+08	1.52E+08	1.38E+08	1.25E+08	1.12E+08
1.23E+08	1.44E+08	1.32E+08	1.21E+08	1.09E+08	9.76E+07
1.09E+08	1.27E+08	1.17E+08	1.06E+08	9.62E+07	8.59E+07
9.65E+07	1.13E+08	1.04E+08	9.44E+07	8.54E+07	7.63E+07
8.62E+07	1.01E+08	9.25E+07	8.44E+07	7.63E+07	6.82E+07

1.20E+00	1.30E+00	1.40E+00	1.50E+00	1.60E+00	1.70E+00
2.33E+08	2.01E+08	1.70E+08	1.38E+08	1.07E+08	7.55E+07
1.90E+08	1.64E+08	1.39E+08	1.13E+08	8.72E+07	6.16E+07
1.58E+08	1.36E+08	1.15E+08	9.38E+07	7.25E+07	5.11E+07
1.33E+08	1.15E+08	9.71E+07	7.91E+07	6.11E+07	4.32E+07
1.14E+08	9.84E+07	8.30E+07	6.77E+07	5.23E+07	3.69E+07
9.84E+07	8.51E+07	7.18E+07	5.85E+07	4.52E+07	3.19E+07
8.60E+07	7.43E+07	6.27E+07	5.11E+07	3.95E+07	2.79E+07
7.57E+07	6.55E+07	5.53E+07	4.50E+07	3.48E+07	2.46E+07
6.72E+07	5.81E+07	4.90E+07	4.00E+07	3.09E+07	2.18E+07
6.00E+07	5.19E+07	4.38E+07	3.57E+07	2.76E+07	1.95E+07

1.80E+00	1.90E+00	1.94E+00
4.41E+07	1.26E+07	0.00E+00
3.59E+07	1.03E+07	0.00E+00
2.98E+07	8.52E+06	0.00E+00
2.52E+07	7.19E+06	0.00E+00
2.15E+07	6.15E+06	0.00E+00
1.86E+07	5.32E+06	0.00E+00
1.63E+07	4.65E+06	0.00E+00
1.43E+07	4.09E+06	0.00E+00
1.27E+07	3.63E+06	0.00E+00
1.14E+07	3.25E+06	0.00E+00

x1 (m)	Mab (Nm)	x2 (m)	Mbc (Nm)
0.00E+00	0.00E+00	1.00E+00	8.33E+03
1.00E-01	8.33E+02	1.10E+00	6.67E+03
2.00E-01	1.67E+03	1.20E+00	5.00E+03
3.00E-01	2.50E+03	1.30E+00	3.33E+03
4.00E-01	3.33E+03	1.40E+00	1.67E+03
5.00E-01	4.17E+03	1.50E+00	-7.40E-12
6.00E-01	5.00E+03		
7.00E-01	5.83E+03		
8.00E-01	6.67E+03		
9.00E-01	7.50E+03		
1.00E+00	8.33E+03		

ARM HEIGHT (h)(m)	γ/I
1.00E-01	3.49E+04
1.10E-01	2.84E+04
1.20E-01	2.36E+04
1.30E-01	1.99E+04
1.40E-01	1.70E+04
1.50E-01	1.47E+04
1.60E-01	1.29E+04
1.70E-01	1.13E+04
1.80E-01	1.01E+04
1.90E-01	9.00E+03

0.00E+00	1.00E-01	2.00E-01	3.00E-01	4.00E-01	5.00E-01
0.00E+00	2.91E+07	5.82E+07	8.72E+07	1.16E+08	1.45E+08
0.00E+00	2.37E+07	4.74E+07	7.11E+07	9.48E+07	1.19E+08
0.00E+00	1.97E+07	3.94E+07	5.91E+07	7.88E+07	9.84E+07
0.00E+00	1.66E+07	3.32E+07	4.98E+07	6.65E+07	8.31E+07
0.00E+00	1.42E+07	2.84E+07	4.26E+07	5.68E+07	7.10E+07
0.00E+00	1.23E+07	2.46E+07	3.69E+07	4.91E+07	6.14E+07
0.00E+00	1.07E+07	2.15E+07	3.22E+07	4.29E+07	5.37E+07
0.00E+00	9.45E+06	1.89E+07	2.84E+07	3.78E+07	4.73E+07
0.00E+00	8.39E+06	1.68E+07	2.52E+07	3.36E+07	4.19E+07
0.00E+00	7.50E+06	1.50E+07	2.25E+07	3.00E+07	3.75E+07

6.00E-01	7.00E-01	8.00E-01	9.00E-01	1.00E+00	1.10E+00
1.74E+08	2.04E+08	2.33E+08	2.62E+08	2.91E+08	2.33E+08
1.42E+08	1.66E+08	1.90E+08	2.13E+08	2.37E+08	1.90E+08
1.18E+08	1.38E+08	1.58E+08	1.77E+08	1.97E+08	1.58E+08
9.97E+07	1.16E+08	1.33E+08	1.50E+08	1.66E+08	1.33E+08
8.52E+07	9.94E+07	1.14E+08	1.28E+08	1.42E+08	1.14E+08
7.37E+07	8.60E+07	9.83E+07	1.11E+08	1.23E+08	9.83E+07
6.44E+07	7.51E+07	8.58E+07	9.66E+07	1.07E+08	8.58E+07
5.67E+07	6.62E+07	7.56E+07	8.51E+07	9.45E+07	7.56E+07
5.03E+07	5.87E+07	6.71E+07	7.55E+07	8.39E+07	6.71E+07
4.50E+07	5.25E+07	6.00E+07	6.75E+07	7.50E+07	6.00E+07

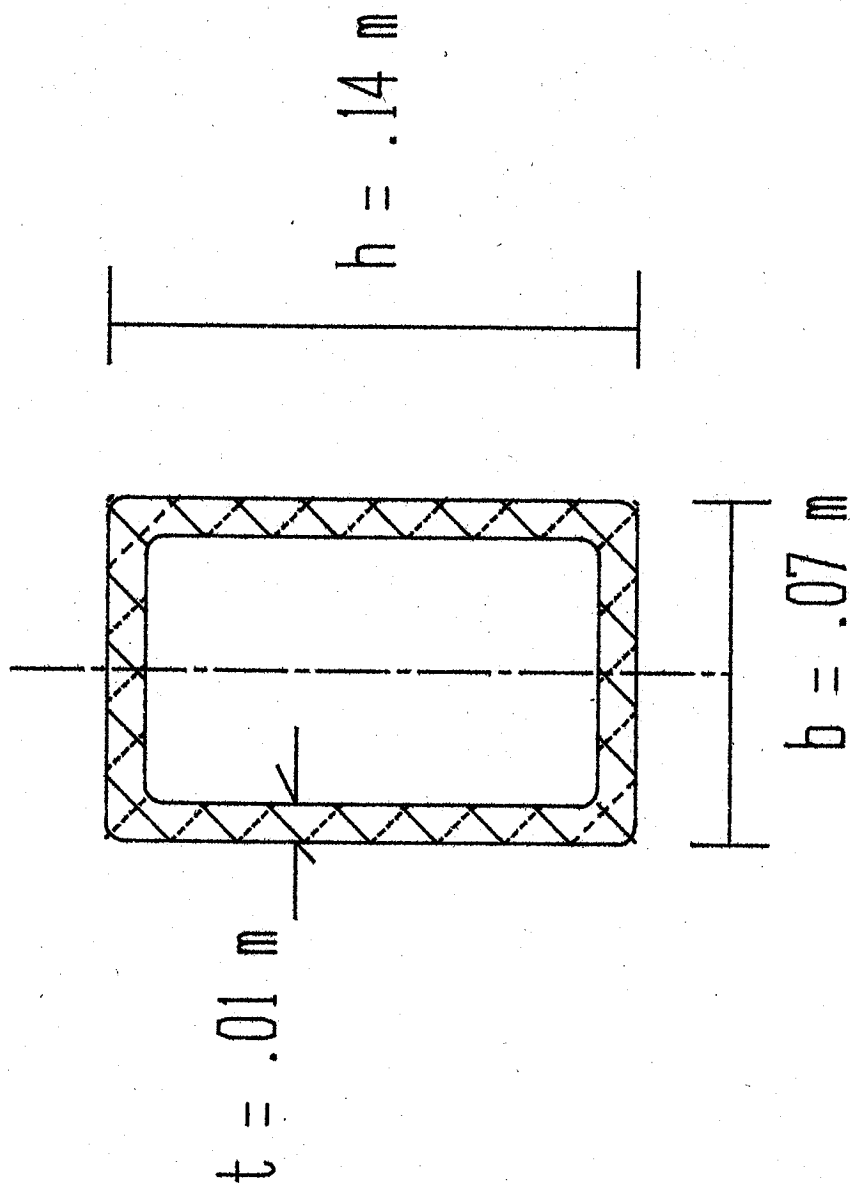
1.20E+00	1.30E+00	1.40E+00	1.50E+00
1.74E+08	1.16E+08	5.82E+07	-2.58E-07
1.42E+08	9.48E+07	4.74E+07	-2.11E-07
1.18E+08	7.88E+07	3.94E+07	-1.75E-07
9.97E+07	6.65E+07	3.32E+07	-1.48E-07
8.52E+07	5.68E+07	2.84E+07	-1.26E-07
7.37E+07	4.91E+07	2.46E+07	-1.09E-07
6.44E+07	4.29E+07	2.15E+07	-9.53E-08
5.67E+07	3.78E+07	1.89E+07	-8.40E-08
5.03E+07	3.36E+07	1.68E+07	-7.45E-08
4.50E+07	3.00E+07	1.50E+07	-6.66E-08

CROSS-SECTION
OF THE SECONDARY AXIS

The cross-section of the arms should have a resistance to moments around both axis. Last quarter's design with rounded ends does not handle moments around the secondary axis very well.

7 The secondary axis would be the one shown below.

The moment of inertia across last quarters secondary axis causes a normal stress 1.5 times greater than the rectangle design. Therefore, the rectangle design is chosen to assure torsion or bending across the secondary axis does not effect the arms.



Cross-sectional view of
arm member

The calculations for the stresses and moments of inertia in last quarter's cross-section are shown below.

LAST QUARTER CROSS-SECTION

$$I = 2(B \cdot T^3 / 12 + A \cdot C^2) + (PI / 64) \cdot (D^4 - d^4)$$

$$T = \text{THICKNESS} = .01 \text{ m}$$

$$B = \text{BASE} = .06 \text{ m}$$

$$D = \text{OUTER EDGE DIA.} = .04 \text{ m}$$

$$A = \text{CROSS-SECTION AREA} = .0003 \text{ m}^2$$

$$C = \text{CENTER TO EDGE DIST.} = .02 \text{ m}$$

$$d = \text{INNER EDGE DIA.} = .03 \text{ m}$$

σ = NORMAL STRESS FROM BENDING

$$= \text{MOMENT} \cdot C / \text{MOMENT OF INERTIA} = MC / I$$

$$\text{APPROXIMATE } M = \text{FORCE} \cdot 1 \text{ m} = F \text{ (Nm)}$$

CALCULATING,

$$I = 6.3 \cdot 10^{-7}$$

$$\sigma = 31.950 \cdot F$$

The rectangular cross-section calculations can be shown below. The results show a better resistance to the moment.

RECTANGULAR CROSS-SECTION

$$I = H*B^3/12 - h*b^3/12$$

$$B = \text{OUTER BASE} = .07 \text{ m}$$

$$H = \text{HEIGHT} = .14 \text{ m}$$

$$b = \text{INNER BASE} = .06 \text{ m}$$

$$h = \text{INNER HEIGHT} = .13 \text{ m}$$

$$\text{SIGMA} = \text{NORMAL STRESS} = MC/I$$

CALCULATING,

$$I = 1.8*10^{-6}$$

$$\text{SIGMA} = 19,000 * F$$

THEREFORE, THE SECONDARY AXIS OF THE RECTANGULAR MEMBER IS STRONGER THAN THE SECONDARY AXIS OF LAST QUARTER'S DESIGN. THEREFORE, THE "TORSIONAL LOAD" CAN BE BETTER WITHSTOOD.

COMPRESSION

Local buckling may occur at the high loaded cross-sections. The highest load that occurs is at the maximum moment point. This point is at the hydraulic intersection of the members. Local compression in aluminum plates can be used to approximate the compression of the cross-section. This will give the length of the joint connection needed to spread the force out to protect against local buckling.

The equations used for the required dimensions are shown below. The information is taken from Aluminum Alloy Structures, by Federico M. Mazzolani. The plastic region is taken to be the range for the member calculations.

$$b/t = (PI*(K*E)^{.5})/((12*(1-V^2)*SIGMA)^{.5})$$

LET SIGMA = YEILD STRENGTH = 390/2PLATES = 185N/m²

b = WIDTH OF PLATE

t = THICKNESS OF PLATE

PI = 3.14

K = ENDURANCE LIMIT

V = POISSON'S RATIO

E = MODULUS OF ELASTICITY

USING FIGURE 7.109 IN ALUMINUM ALLOY STRUCTURES, THE b/t RATIO CAN BE FOUND.

$$b/t = 10 \text{ FOR THE SIGMA OF } 185 \text{ N/mm}^2$$

$$t = .01 \text{ m}$$

$$\text{THEREFORE, } b = .01 \times 12 = .01 \text{ m}$$

Fig. 7.109 Values of b/t

FO.2	b/t		
(N*mm ⁻²)	(a)	(b)	(c)
80	31.8	18.3	56.2
125	25.5	14.7	45.0
160	22.5	13.0	39.8
200	20.1	11.6	35.6
260	17.6	10.2	31.2
280	17.0	9.8	30.1

*(note: Figure 7.109 is taken from Aluminum Alloy Structures by F.M.Mazzolanni, 1985)

SHEAR

Most of the shear takes place at the compression analysis above. If one wants a simple idea of the shear at the previous cross-section, an estimate of the maximum shear stress must be estimated. If a safety factor of 3 is used the calculations can be shown below.

$$\begin{aligned} TM &= \text{MAXIMUM SHEAR STRESS} = \text{YIELD ST.}/2N \\ &= (390 \times 10^6 \text{ N/m}^2)/2 \times 3 = 65 \times 10^6 \text{ N/m}^2 \end{aligned}$$

$$\begin{aligned} T &= V/\text{CROSS-SECTION} = 25\text{KN}/(2 \times .01 \times (.7 + 1.4)) \\ &= 6 \times 10^5 \text{ N/m}^2 \end{aligned}$$

$$TM \gg T$$

APPENDIX 2

POWER SYSTEM COMPARISON

POWER SYSTEM COMPARISON

ELECTRIC MOTOR

NASA has used the samarium-cobalt, permanent-magnet, brushless dc motor on the Space Shuttle Orbiter. Delco Electronics designed, fabricated, and tested the motor to suit NASA's constraints, which are the same as ours.

The samarium-cobalt reduces motor weight and increases the efficiency. The motor is rated at 17 horsepower and can be cooled by fluid through the stator windings. The efficiency is rated from 89% to 95% depending on the load applied, and the endurance is estimated at 5 years. This means that the motor needs to be replaced only once during the ten years life expectancy of the digger.

ACTUATOR SYSTEM

The decision for an actuator system was difficult to make. Electromechanics is becoming more efficient with current technology, but hydraulics are still popular in lunar design. The primary benefit of electromechanics is the fact that no fluid is involved. The "pros" and "cons" of each system can be listed in tabular form. (See Figure 2). Since the hydraulics are more adaptable to the Moon, a hydraulic actuator system is chosen for the digger.

ACTUATOR COMPARISON

<u>HYDRAULIC</u>	<u>ELECTROMECHANICAL</u>
+EASILY CONTROLLED	+EASILY CONTROLLED
-LEAKAGE OF FLUID	+NO FLUID
+INSTANT BRAKING	-DYNAMIC BRAKING
-POSSIBLE FLUID FREEZE	+NO FLUID
-WEAR AND DUST	-WEAR AND DUST
+POWER/WEIGHT RATIO	-1/3 HYDRAULIC RATIO
+CONSTANT SPEED VS. TORQUE	-DECREASING TORQUE WITH SPEED
+HIGH EFFICIENCY(95%)	-EFFICIENCY(70%)
+NO GEARS INVOLVED	-POSSIBLE FREEZING OF GEARS

+ PRO

- CON

FIGURE 2

APPENDIX 3

HYDRAULICS

HYDRAULIC SYSTEM

Hydraulic actuators will provide the necessary forces to power the Lunar Digger. The digger requires a total of eight actuators: one rotary and seven linear. The location of the actuators are shown in figure (III-1). These actuators consist of:

- 1-a rotary actuator to pivot the digger around the shoulder pin
- 2-two linear actuators in parallel connecting the shoulder to the upper arm
- 3-a linear actuator connecting the upper arm to the lower arm
- 4-a linear actuator connecting the end effector to the lower arm
- 5-a linear actuator which will pivot one bucket arm about the end effector
- 6-a linear actuator to pivot each bucket

COMPONENTS

A schematic diagram of the hydraulic system of the Lunar Digger is shown in figure (III-2). Low pressure hydraulic fluid is stored in a fluid reservoir. A hydraulic pump will take the fluid from the reservoir, through a filter, and pressurize it to 24,000 kPa. The fluid is first pumped through a system pressure relief valve. This valve is used as a safety precaution. If the system pressure exceeds a specified pressure, for example hitting a rock while pecking, the

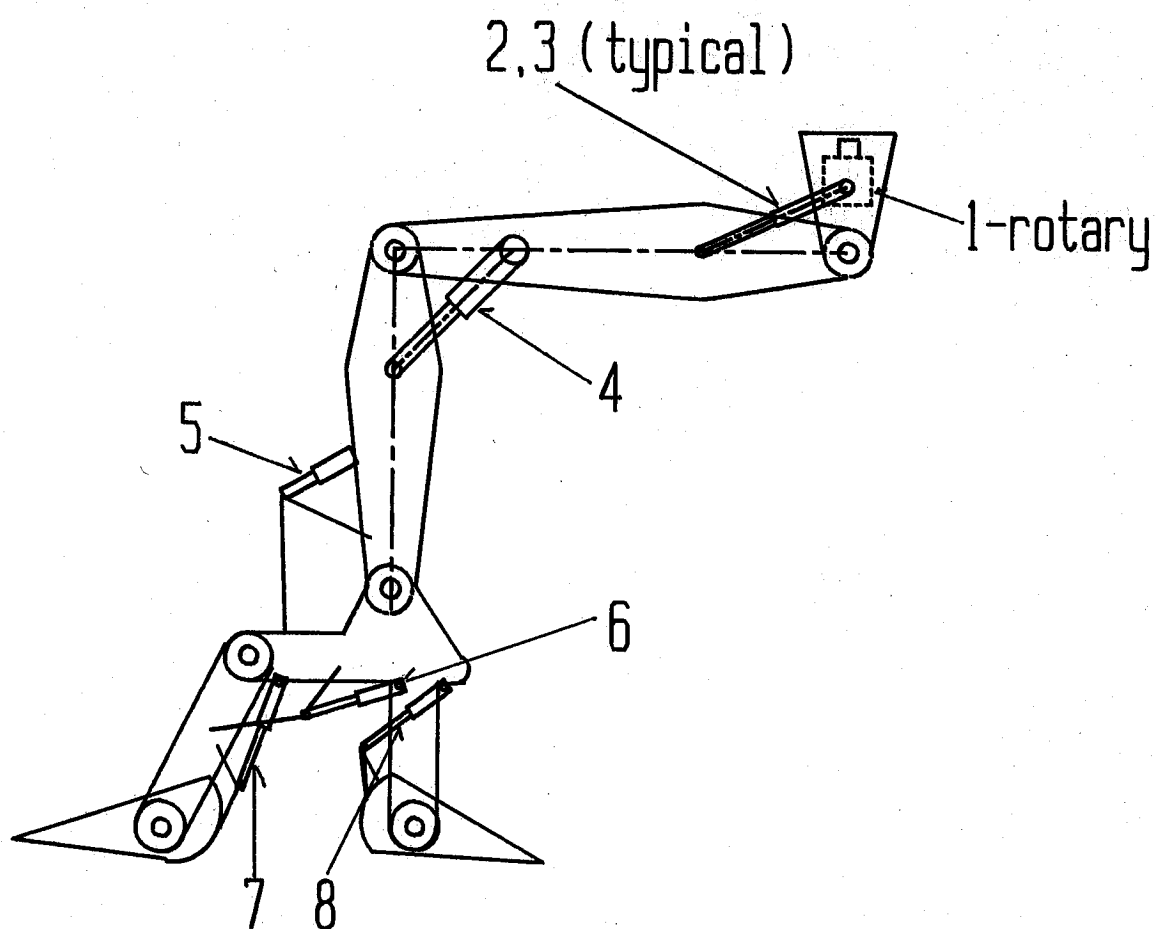
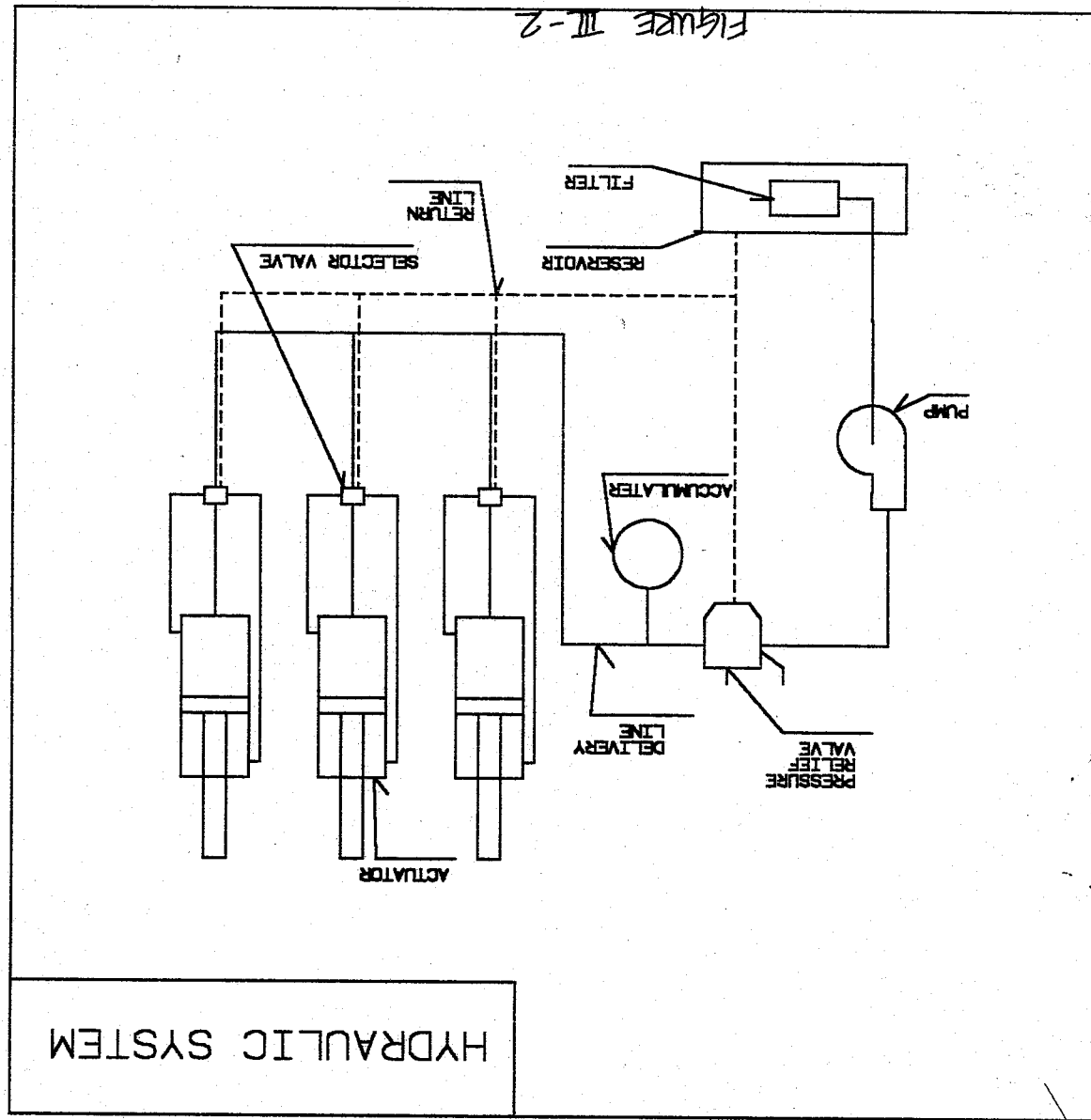


Figure III-1.
Location of actuators



relief valve will send the pressurized fluid back to the reservoir. The pressurized fluid is stored in an accumulator until fluid is needed to activate an actuator. When a force is needed the selector valve is switched to allow fluid to flow to the side of the actuator which requires the pressurized fluid. The fluid from the opposite side of the actuator is forced out of the cylinder, through the selector valve, and drained to the fluid reservoir. The pressurized fluid acting against the the piston causes the force required by the actuator.

REQUIRED FORCES

The first step in determining the particular components needed to power the Lunar Digger is to calculate the necessary forces required of the actuators. The maximum lifting forces of the shoulder to arm actuators and the upper arm to lower arm actuator occurs when the arm is holding two full buckets out horizontally. The moon weight of two full buckets of soil is 1820 N, and the weight of the end effector and the two buckets is 500 N. Using this information along with the weights of the upper and lower arms, which are 22 N and 12 N respectfully, static force analysis determines that the arm to arm actuator must deliver a force of 35,000 N and each of the shoulder to upper arm actuators must deliver a force of 7900 N.

FORCE PROGRAM

In order to effectively choose the correct size actuators, we wrote a computer program which would calculate extending and retracting forces depending on several system pressures, ranging from 7000 kPa to 41,000 kPa. The force delivered by the actuator also depends on the area on which the pressure is acting; therefore, the program also calculates forces of any desired bore diameters. The program also calculates the power required to move an actuator at a given velocity. The power will be necessary in order to choose a motor for the system. The equations used in the program are as follows:

$$F = \text{pressure} \times \text{PI} \times (D)^2 / 4 \quad (1)$$

$$F = \text{pressure} \times \text{PI} \times (D^2 - d^2) / 4 \quad (2)$$

$$\text{Cylinder Flow Rate} = 3.117 \times \text{velocity} \times \text{PI} \times (D)^2 / 4 \quad (3)$$

$$\text{Horsepower} = \text{Cyl Flow Rate} \times \text{pressure} / 1714 \quad (4)$$

SYSTEM PRESSURE/ACTUATOR SIZING

From the computer generated results, which are shown in table (III-1), we chose a system pressure of 24,000 kPa. At this pressure, the arm to arm force of 35,000 N can be achieved with an actuator with a bore diameter of 5 cm. At a cylinder velocity of .2 meters per second, this actuator will consume power equal to 7.5 kw. The two actuators in parallel from the shoulder to the upper arm, which require a force of 7900 N , can be achieved by using an actuator with a bore diameter of 2.5 cm. At the same cylinder velocity, these actuators will use 2 kw of power each. The actuator which connects the end effector to the lower arm requires a bore diameter of 2.5 cm and a rod diameter of 1.3 cm. This actuator will produce a net extending force of 12,000 N and retracting force of 9,000 N. The minimum and maximum lengths of this actuator are .75 and 1.5 m, respectively. The bore diameter and rod diameter of the actuator which pivots one of the buckets about the end effector are also 2.5 and 1.3 cm, respectively. The minimum length of this actuator is .5 m and the maximum length is 1 meter. The two actuators which control the bucket have a bore diameter of 3.8 cm and a rod diameter of 1.9 cm. They will have a minimum length of .75 m and a maximum length of 1.5 m. Each will deliver 4.2 kw of power. The rotary actuator, which rotates at a speed of 7.5 rev/min, must deliver a torque equal to 15,000 Nm. This requires an input power of 10.5 kw. The calculations are shown in figure (III-3). The Asea

ACTUATOR

No.:

2 & 3

SYSTEM PRESSURE (kPa)	BORE DIAMETER (cm)	ROD DIAMETER (cm)	BORE AREA (sq cm)	ROD AREA (sq cm)	AREA DIFFERENCE (sq cm)
24000	2.5	1.3	5.0	1.3	3.8
CYLINDER VELOCITY (m/s)	FLOW RATE (gal/min)	POWER OUT (kw)	EXTENDING FORCE (kn)	RETRACTING FORCE (kn)	
0.2	4.9	1.9	12	9	

ACTUATOR

No.:

4

SYSTEM PRESSURE (kPa)	BORE DIAMETER (cm)	ROD DIAMETER (cm)	BORE AREA (sq cm)	ROD AREA (sq cm)	AREA DIFFERENCE (sq cm)
24000	5.0	2.5	20.3	5.1	15.2
CYLINDER VELOCITY (m/s)	FLOW RATE (gal/min)	POWER OUT (kw)	EXTENDING FORCE (kn)	RETRACTING FORCE (kn)	
0.2	4.9	10.0	49	37	

TABLE III-1a

ACTUATOR

No.:

5

SYSTEM PRESSURE (kPa)	BORE DIAMETER (cm)	ROD DIAMETER (cm)	BORE AREA (sq cm)	ROD AREA (sq cm)	AREA DIFFERENCE (sq cm)
24000	2.5	1.3	5.1	1.3	3.8
CYLINDER VELOCITY (m/s)	FLOW RATE (gal/min)	POWER OUT (kw)	EXTENDING FORCE (kn)	RETRACTING FORCE (kn)	
0.2	4.9	1.9	12	9	

ACTUATOR

No.:

6

SYSTEM PRESSURE (kPa)	BORE DIAMETER (cm)	ROD DIAMETER (cm)	BORE AREA (sq cm)	ROD AREA (sq cm)	AREA DIFFERENCE (sq cm)
24000	2.5	1.3	5.1	1.3	3.8
CYLINDER VELOCITY (m/s)	FLOW RATE (gal/min)	POWER OUT (kw)	EXTENDING FORCE (kn)	RETRACTING FORCE (kn)	
0.2	4.9	1.9	12	9	

TABLE III-16

ACTUATOR

No.:

7 & 8

SYSTEM PRESSURE (kPa)	BORE DIAMETER (cm)	ROD DIAMETER (cm)	BORE AREA (sq cm)	ROD AREA (sq cm)	AREA DIFFERENCE (sq cm)
24000	3.8	1.9	11.4	2.9	8.6

CYLINDER VELOCITY (m/s)	FLOW RATE (gal/min)	POWER OUT (kw)	EXTENDING FORCE (kn)	RETRACTING FORCE (kn)
0.2	2.8	4.2	28	21

TABLE II-1c

HORSEPOWER AND TORQUE REQUIREMENTS
OF THE ROTARY ACTUATOR

$$n = (60 \text{ s/min}) * (1\text{rev}/8\text{s}) = 7.5 \text{ rev/min}$$

$$\text{Required torque} = (3\text{m}) * (5000 \text{ N}) = 15,000 \text{ Nm}$$

$$\begin{aligned} \text{Torque} &= (15,000 \text{ Nm}) * (1\text{in}/2.54\text{cm}) * (100\text{cm}/\text{m}) * (1\text{lb}/5\text{N}) \\ &= 120,000 \text{ inlb} \end{aligned}$$

Now, the horsepower is

$$\text{hp} = \text{tn}/63025$$

$$= (120,000 \text{ inlb}) * (7.5 \text{ rev/min}) / 63025$$

$$= 14.1 \text{ hp}$$

$$(14.1 \text{ hp}) * (.7\text{kw}/\text{hp}) = 20 \text{ kw}$$

(The power delivered by the electric motor is 25 kw)

Figure III-3

Hagglunds Ltd corporation manufactures a hydraulic drive of this sort with an efficiency of 94 %. See figure (III-4). Using the cylinder volumes calculated from the actuator dimensions above, the digger will require 200 cubic centimeters of hydraulic fluid. The best hydraulic fluid we found was synthetic based fluids manufactured by Royal Lubricants Company. See figure (III-5). The temperature range for this fluid is from -50 to 200 degrees Celcius, while the other fluids that we researched ranged from -10 to 100 degrees Celcius.

HIGH POWER IN A CONFINED SPACE: ELECTRIC VERSUS HYDRAULIC DRIVES

To many engineers who need controllable power sources, it seems only natural to look at electric drives. Certainly electric motor and controller design has gone through huge leaps in technology over the past few years.

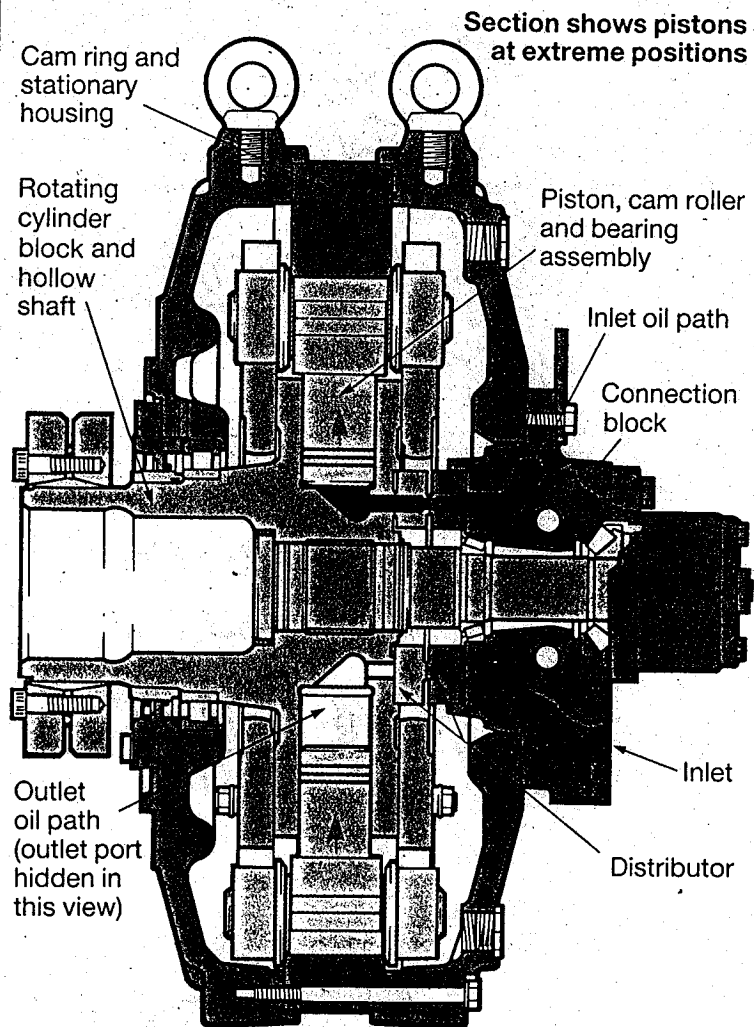
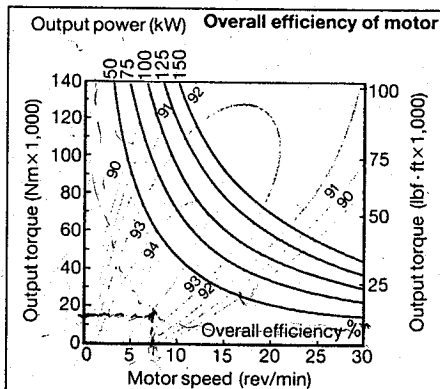
Set against such a background one might question the reasoning behind developing a new hydraulic drive system billed as 'the hydraulic revolution'. However, when one considers that at the highest power levels electric variable speed drives require more than three times as much space than a hydraulic motor—or, put another way, for the same weight can deliver perhaps only a third to half of the power—a strong case can be made for hydraulics.

ASEA Hägglunds have identified the need for durable motors with low-maintenance, soft start, high torque, low speed characteristics, and supplied as part of an integrated drive system. In fact, such a system stands to gain from developments in electronic motor control which allows pump motor speeds to be easily varied under direct electronic control.

With this in mind, we have developed the most compact and powerful direct drive hydraulic motor yet. Called the Marathon range, our designers have found a way of turning a hydraulic motor 'inside out' by using a unique distributor plate.

With up to 160 power strokes per revolution uniform torque output is guaranteed. And the novel distributor design allows forward, reverse or oscillation motion from the shaft. Position control is also possible, allowing the unit to operate as a giant hydraulic stepper motor.

Exact speed control (via a variable speed pump) enables the motor to be matched to the drive line characteristics. For example, where torque is proportional to the square of the speed, as in most processes requiring stirring, agitating or pumping.



The distributor

This vital assembly allows pressurised oil to access and exit from individual pistons in the correct sequence. The design must ensure that the motor can be started from any position, that leakage between inlet and outlet ports to each cylinder is minimised, and that parts remain lubricated to prevent wear.

The illustration shows the components of the distributor—essentially of a face-plate design where the face of a rotating component moves past that of a stationary one 'opening' and 'closing' the ports.

The exact details of the design have to remain secret—patents are pending—however, we can reveal that it does not require seals, that leakage between inlet and outlet ports is prevented, and that leakage (used for lubrication of the parts) is controlled in quantity and direction.

This technology contributes largely to the overall efficiency of the motor, which as our diagram shows, is in the region of 95 per cent.

ASEA HÄGGLUNDS

Asea Hägglunds Ltd

Wakefield 41, Wakefield, West Yorkshire WF2 0XE
Telephone: 0924 826021 Telex: 557252 Telefax: 0924 826146



ROYAL LUBRICANTS COMPANY

MIL-H-
Am

TECHNICAL DATA SHEET

ROYCO 846

ROYCO MICRONIC 846

AIRCRAFT HYDRAULIC FLUID, NON-PETROLEUM BASE, HIGH TEMPERATURE

DESCRIPTION: ROYCO 846 is a disiloxane base hydraulic fluid of low volatility and excellent viscosity - temperature characteristics. It is red-brown in color and contains additives to impart resistance to oxidation, hydrolysis and shear.

USES: ROYCO 846 is intended for use in aircraft hydraulic systems subject to extreme temperature changes, and is designed for operation from -65°F to +400°F.

LIMITATIONS: ROYCO 846 is a synthetic base hydraulic fluid and may adversely affect certain paints and elastomers. Only those materials developed for use with this fluid should be used, unless compatibility studies proves a product to be satisfactory. Royco 846 is not compatible with castor oil base (MIL-H-7644) or petroleum base (MIL-H-5606) hydraulic fluids. Contamination with fluids of this type will substantially shorten its service life. ROYCO 846 should be kept in an inert atmosphere and should be thoroughly protected against moisture.

PACKAGING: ROYCO 846 is available in quart and gallon cans, and 5-gallon and 55-gallon drums. ROYCO MICRONIC 846 is available in quart and gallon cans and 55-gallon-drums. (See particulate contamination levels).

SPECIFICATIONS: ROYCO 846 meets all requirements and is a qualified product under MIL-H-8446B.

PROPERTIES

<u>Test</u>	<u>Requirements</u>	<u>Typical</u>
Viscosity, centistokes, at 400°F	2.5 min.	2.7
210°F	report	7.9
100°F	report	24
-65°F	2500 max.	2400
Vapor Pressure @ 400°F, mm Hg.	5.0 max.	2.6
Autogenous Ignition Temp. °F.	700 min.	815
Flash Point, COC, °F.	395 min.	400
Pour Point, °F.	-75 max.	<-75
Acid Number, mg KOH/gm	0.2 max.	0.05
Water Content, %	0.01 max.	Nil
Toxicity	Non-hazardous	Pass
Appearance	Clear, no sediment	Light red-brown, pass

FIGURE II-5a

58.

Hydrolytic Stability, 200°F. for 48 hrs.		
Corrosion to copper, wt. change, mg/cm ²	+0.5	+0.01
Color, ASTM	I max.	Pass
Acid Number Increase, mg. KOH/gm.		#
water layer	0.3 max.	+0.05
oil layer	0.5 max.	+0.08
Viscosity, change at 210°F., %	+20	1
Insolubles, %	0.5 max.	0.1
Oxidation and Corrosion Stab. @ 400°F, 72 hrs.		
Corrosion, wt. change, mg/cm ²		
Silver	+0.2	+0.02
Steel	+0.2	0.00
Aluminum	+0.2	0.00
Copper	+0.4	+0.02
Appearance of Metals	No pits, etching, corrosion	Pass
Oxidation		
Viscosity change at 210°F, %	+35	-24
Acid Number change, mg. KOH/gm	I.0 max.	+0.35
Appearance	NO gum or insolubles	Pass
Swelling of Synthetic Rubber "S"		
at 250°F, %	15-25	18
Storage Stab. 1 yr. at room temp.	No separation	Pass
Low Temp. Stability @ -65°F, for 72 hrs.	No gel, crystals or solid	Pass
Foaming at 200°F.		
Total Volume of Foam, ml	60C max.	520
Collapse Time, minutes,	10 max.	7
Shear Stability, 5,000 cycles at 275°F.	Pass	Pass
Wear Properties, 3,000 psi at 275°F for 200 hrs.	Report	Pass
Compatibility with all fluids on QPL-8446	Pass	Pass

TYPICAL PHYSICAL PROPERTIES

Temperature, °F.	Specific Heat, BTU/LB/°F.	Thermal Conductivity, BTU/sq.ft/hr/°F/ft	Density, gm./cc.
0	--	--	0.950
100	0.48	0.085	0.911
200	0.52	0.082	--
300	0.56	0.077	0.835
400	0.66	0.057	0.782

gm/cc

Temperature, °F.	Bulk Modulus, Acoustic Pressure, PSI	Bulk Modulus, PSI
100	0	170,000
	1000	182,000
	3000	205,000
	5000	225,000
250	0	100,000
	1000	113,000
	3000	122,000
	5000	155,000
400	0	60,000
	1000	74,000
	3000	100,000
	5000	125,000

PARTICULATE CONTAMINATION LEVELS

*Particulate Contamination Level, Particle Size, Microns

ROYCO 846

ROYCO Micronic 846

Quarts and Gallons, Maximum Drums, 55 gals, Maximum

5 - 15

4,000

10,000

15 - 25

Not

400

4,000

25 - 50

Defined

200

1,000

50 - 100

25

50

100+

5

15

*Particulate contamination determined by method ARP598.

FIGURE III-56



ROYAL LUBRICANTS COMPANY

COMMERCIAL

TECHNICAL DATA SHEET

ROYCO 820X

DI SILOXANE BASE AIRCRAFT HYDRAULIC FLUID

DESCRIPTION: ROYCO 820X is a disiloxane base (synthetic) hydraulic fluid having good viscosity temperature characteristics coupled with extreme low volatility. This fluid is brownish-red in color and contains additives to impart resistance to oxidation, corrosion and hydrolysis. ROYCO 820X is shear stable.

USES: ROYCO 820X is intended for use in newly designed aircraft and missile hydraulic systems where temperatures will be encountered exceeding 350°F, but where operation at -65°F is still required. Its use as a heat transfer media is suggested.

LIMITATIONS: ROYCO 820X is a synthetic base fluid and may adversely affect paint and rubber. This material is intended for those hydraulic systems designed for MLO 8200 fluids, its use in other systems should not be considered unless proven satisfactory by performance tests.

PACKAGING: ROYCO 820X is available in 5 gallon and 55 gallon drums.

SPECIFICATION: ROYCO 820X meets all requirements as established by the experimental MLO 8200 formulation.

TYPICAL PHYSICAL PROPERTIES

Viscosity Centistokes @

400°F
210°F
100°F
-65°F

3.7
11.1
32
2400

Pour Point

Below -100°F

Low Temp Stability (72 hrs. @ -65°F)

Clear Liquid no haze or crystals

Acid Number

0.01

Flash Point

420°F

Fire Point

470°F

Vapor Pressure, 400°F

1.0 mm Hg.

Autogenous Ignition

750°F min.

Rubber Swell (S Rubber) 70 hrs. @ 250°F

7.0 %

(26C Rubber) 148 hrs. @ 400°F

10%

Hydrolytic Stability (48 hrs. @ 200°F)

Wt. Change copper mg/sq.cm.

-0.02

Copper Appearance

Slight dulling

Acid Number change Oil Layer

0.08

H₂O Layer

0.02

Viscosity change @ 210°F

+1.8%

Insolubles)

0.05%

FIGURE III-5c

60

FOAMING - Total Volume Foam

Collapse Time

Storage Stability - 1 year

Oxidation - Corrosion Stability (72 hr. @ 400°F)

Corrosion, Wt. Change mg/sq. cm, Appearance

Silver

Steel

Aluminum

Copper

Oxidation

Viscosity Change @ 210°F

Acid Number Change

Insolubles

Density @ -65°F

@ 400°F

Specific Heat (BTU/lb/°F)

@ 0°F

@ 100°F

@ 200°F

@ 300°F

@ 400°F

Compressibility (in²/lb.) 77°F, 300 psig

Shear Stability

Pump Lubricating

450 ml

3-3/4 min.

Stable

-0.04 Bright, Passes

-0.02 Staining, Passes

Nil Staining, Passes

Nil Staining, Passes

-10%

0.4

None

0.993

0.783

0.407

0.421

0.433

0.456

0.478

5.2X10⁻⁶

Satisfactory

Satisfactory

FIGURE III-5d

APPENDIX 4

Heat Transfer

APPENDIX 4

HEAT TRANSFER CALCULATIONS

Heat input into the digger mechanism was assumed to be from solar radiation and the heat output from the electric motor and the hydraulic pump due to inherent inefficiencies. The heat flux from the electric motor was specified at 822 watts. The waste heat flux from the hydraulic system was calculated to be 1343 watts. ($Q = 12 \text{ hp} \times 746 \times .15 = 1343$). The heat flux expelled by the radiator is a black body radiation problem; therefore, $q = A(\sigma)(\epsilon)(\text{Temp. of Al}^4 - \text{Temp. of space}^4)$. The values for these quantities are: $\sigma = 5.6697\text{e-}8 \text{ W/m}^2 \text{ K}^4$; $\epsilon = 0.8$; and temperature of deep space = 210 K. This information was plugged into Lotus to produce a graph comparing the temperature of the space radiator to the area needed to dissipate excess heat. (See Figure 4.1.) The temperature of the hydraulic fluid was analyzed using the laminar flow forced convection equation: $T_w - T_b = (11/48)(qD/K)$. This equation was plugged into Lotus to analyze changes in fluid temperature as a result of changing wall temperatures, T_w , and heat flux, q . The bulk temperature, T_b , is the temperature in a pipe experiencing uniform heat flux after the fluid and temperature profiles of the fluid have stabilized. (See Figures 4.2-5.) Figure 4.2 demonstrates the need for insulation coating. The hydraulic fluid would otherwise

experience temperatures below acceptable range during the cold period. Figure 4.3 reinforces this fact by showing that a greater output than input of heat occurs during the cold period. As the temperature increases the difference between heat lost and gained increases in an almost exponential fashion, (Figure 4.4), until reaching a point where fluid temperature decreases with increasing arm temperature. (See Figure 4.5.)

WASTE HEAT UTILIZATION

The use of waste heat to produce power was considered to be a viable means of producing power. Dr. Shelton mentioned using a Brayton steam cycle to convert excess heat to power. Waste heat can also be channeled into a fuel cell. The problem with using waste heat is that the space radiator panel would have to be considerably larger in order to expell waste heat. A Brayton steam cycle would also occupy considerable space and weight and could be only used during daytime. The waste heat will be used to maintain the fluid temperature over 210 Kelvin during the cold periods. The piping system for the digger mechanism circulates heat uniformly to both sides of each arm thereby maintaining a relatively uniform arm temperature.

ALTERNATE POSITIONING MECHANISMS

Two different positioning mechanisms were being considered. Case 1 uses a crank-follower type mechanism to rotate the panel from beneath the walker to a position to its side. (See Figure 4.6.) Case 2 uses a scissors mechanism to extend the panel up the middle to the outside of the walker. (See Figure 4.7.) Case 1 uses an electric motor to move the each crank arm and to adjust the steel wire which alters the tilt angle of the panel. In case of failure of the steel wire, the linkages can withstand the weight of the panel. This design also has the advantage of easy interchangeability with other panels and no risk of damage to walker if linkages break. Case 2 limits design to a certain maximum size and can damage the walker if one of its linkages break. A more powerful pump would also be required in order for the fluid to be pumped upwards. This design is more complex and heavier than Case 1. Case 1 was chosen for simplicity, ease of maintenance and use, and safety.

ALTERNATE HEAT EXCHANGER CONCEPTS

Other methods of extracting heat from the digger mechanism were considered. A solid adsorbent heat exchanger was dropped from consideration when it was learned from Dr. Shelton that a heat source and sink is needed for this heat exchanger to work. The lack of a good thermal sink made conventional heat exchangers impractical. The only possible heat sink available, except for

deep space, is the soil itself which is supposed to be at 227 K. Since the soil is a great insulator, a relatively low heat flow rate is expected thereby not expelling much heat. Positioning this mechanism in a position that did not constrain the motion of the digger arm.

SPACE RADIATOR LINKAGES SIZING

The cantilever beam program, Table 2, was used on the HP 41C to evaluate forces at the endpoints and to calculate the maximum deflection of different sized members. Various values for the moment at the fixed end of the crank were used to optimize the length. The two cantilever beams were designed to withstand the full load of the space radiator, 443 Newtons. The steel wire normally relieves part of this load while tilting the panel in the desired direction. The steel wire lifts the panel slightly to unlock the brace holding the crank and follower together and reels in to a position necessary to hold the panel in the desired position.

SPACE RADIATOR

area vs. temp.

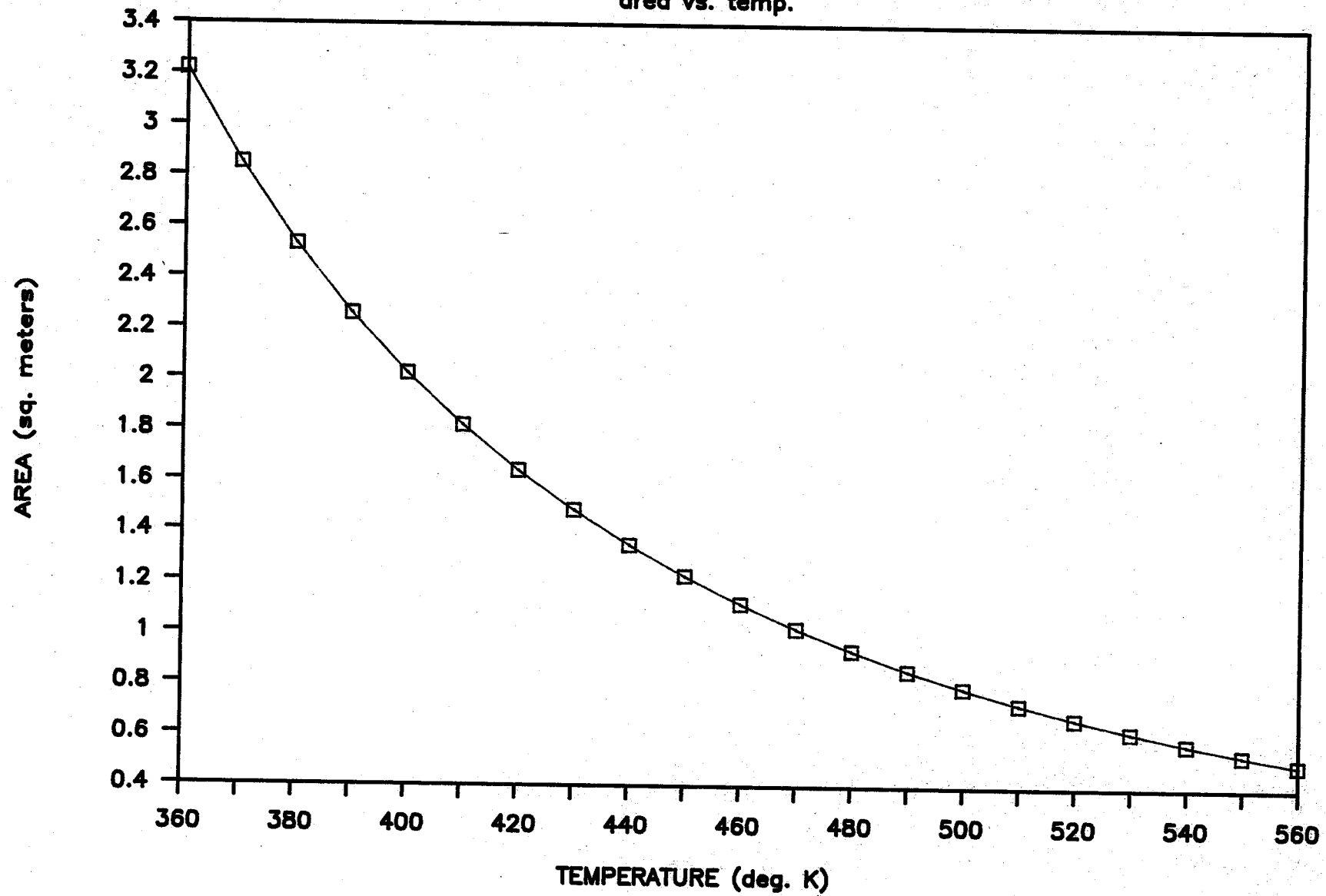


FIGURE 1

DIGGER ARM

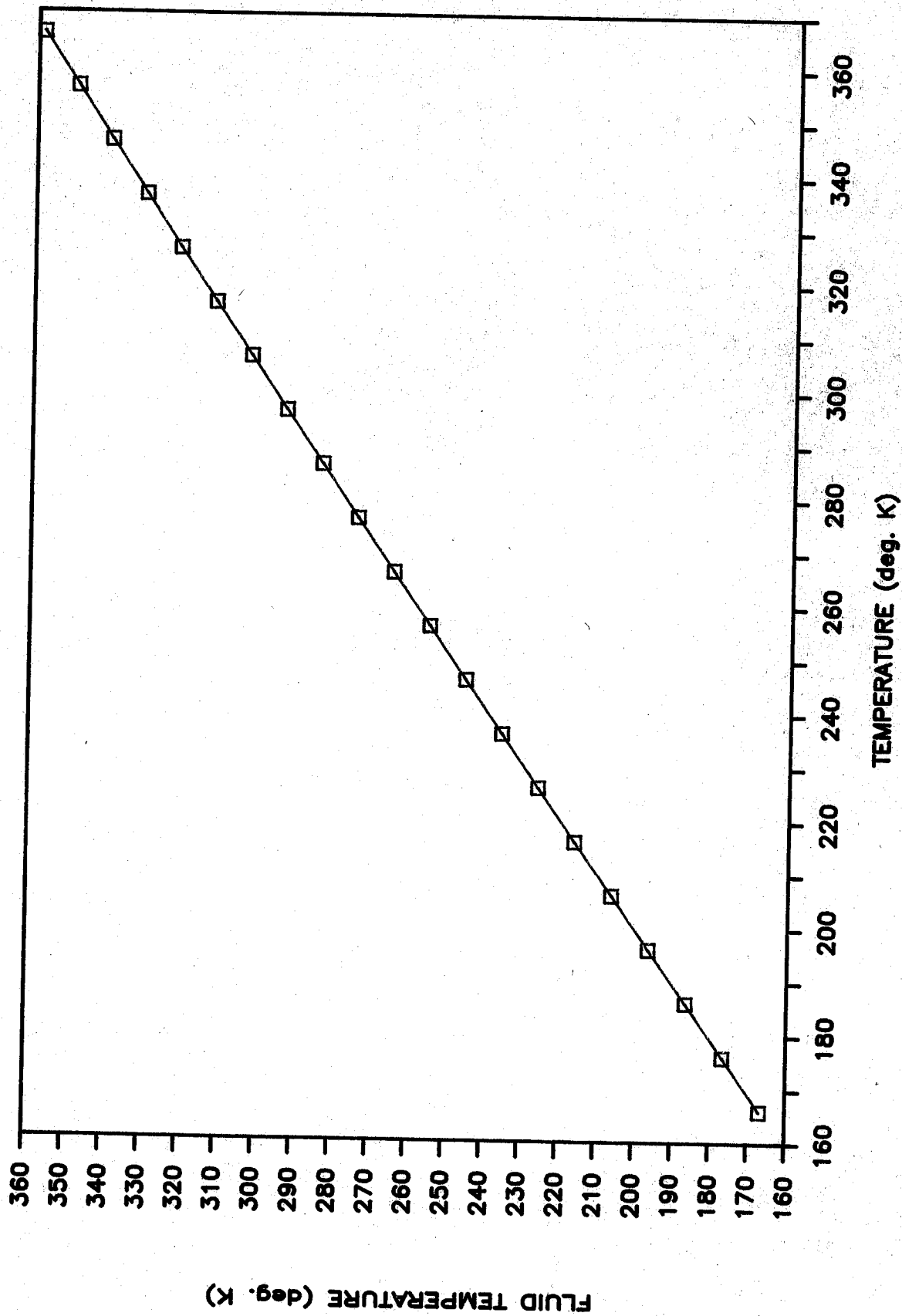


FIGURE 2

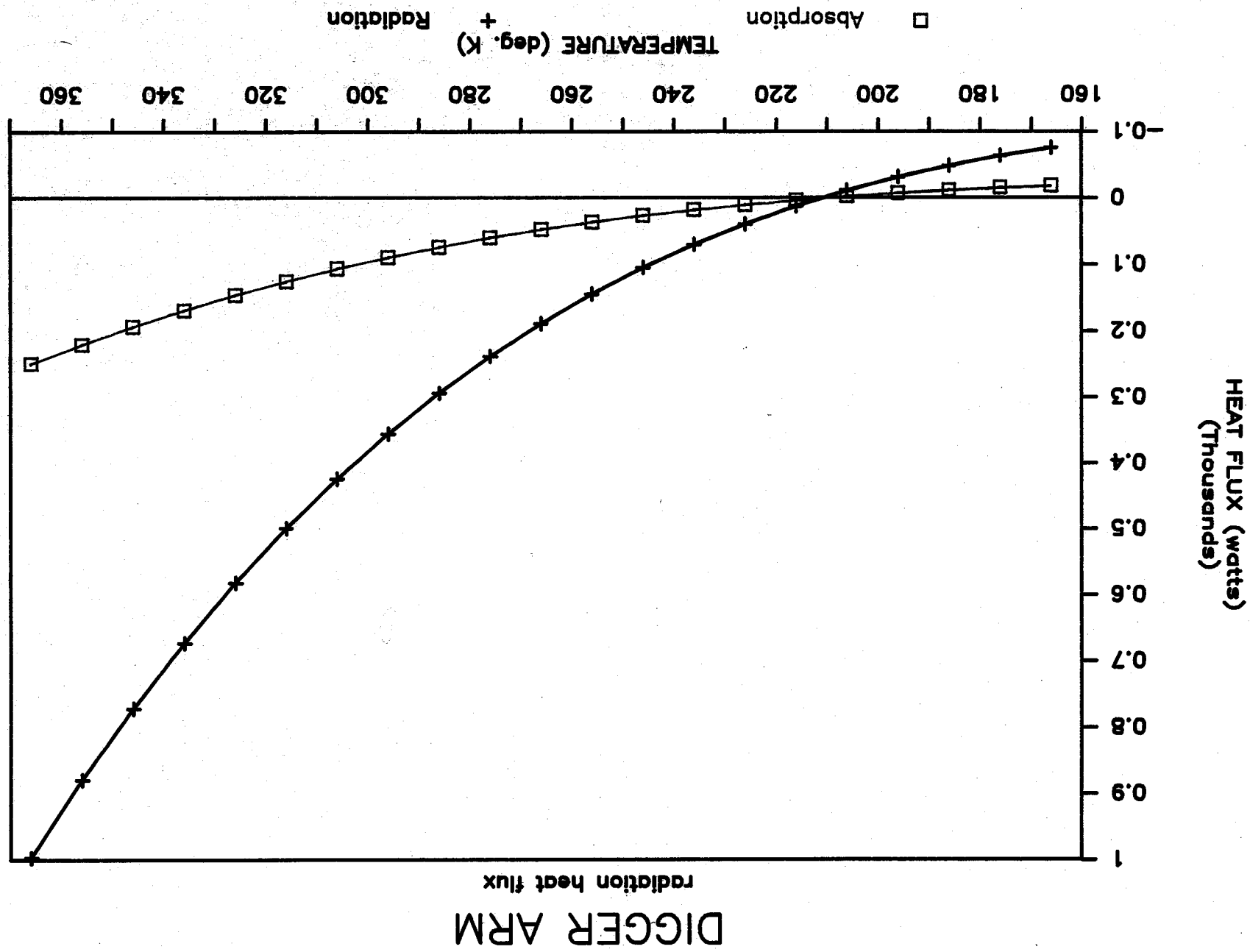


FIGURE 3

70

DIGGER ARM

RADIATION HEAT FLUX

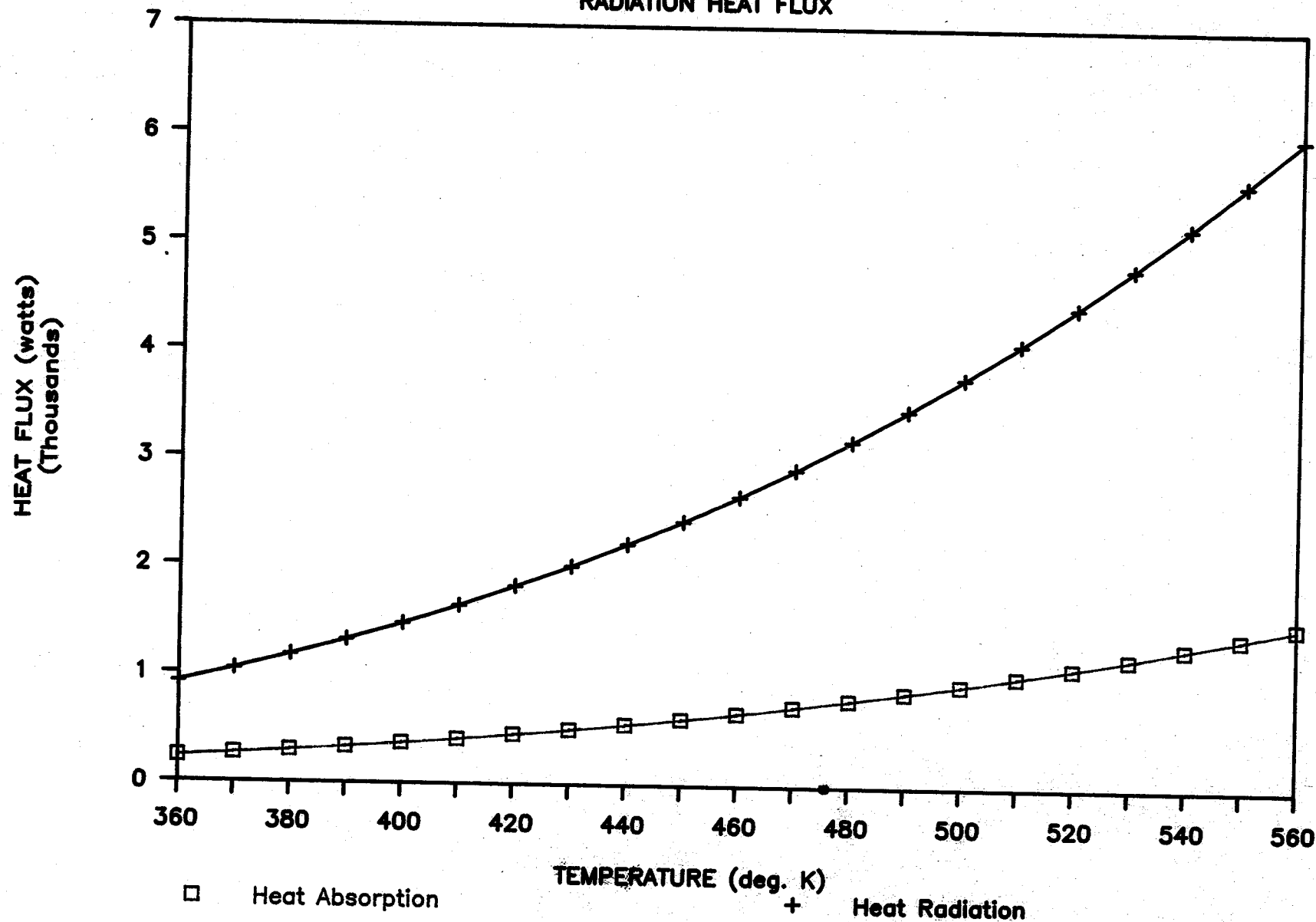
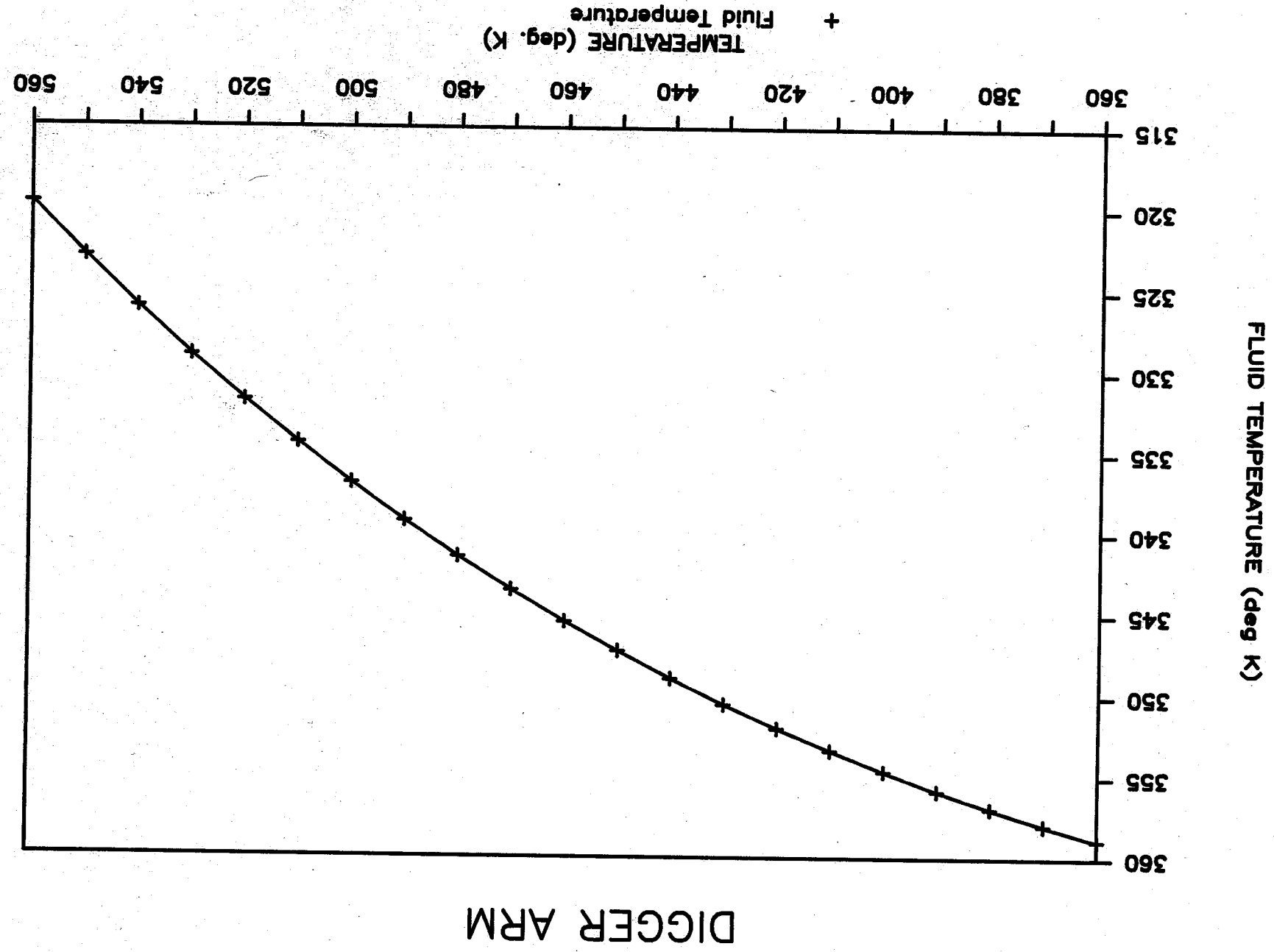


FIGURE 4

FIGURE 5



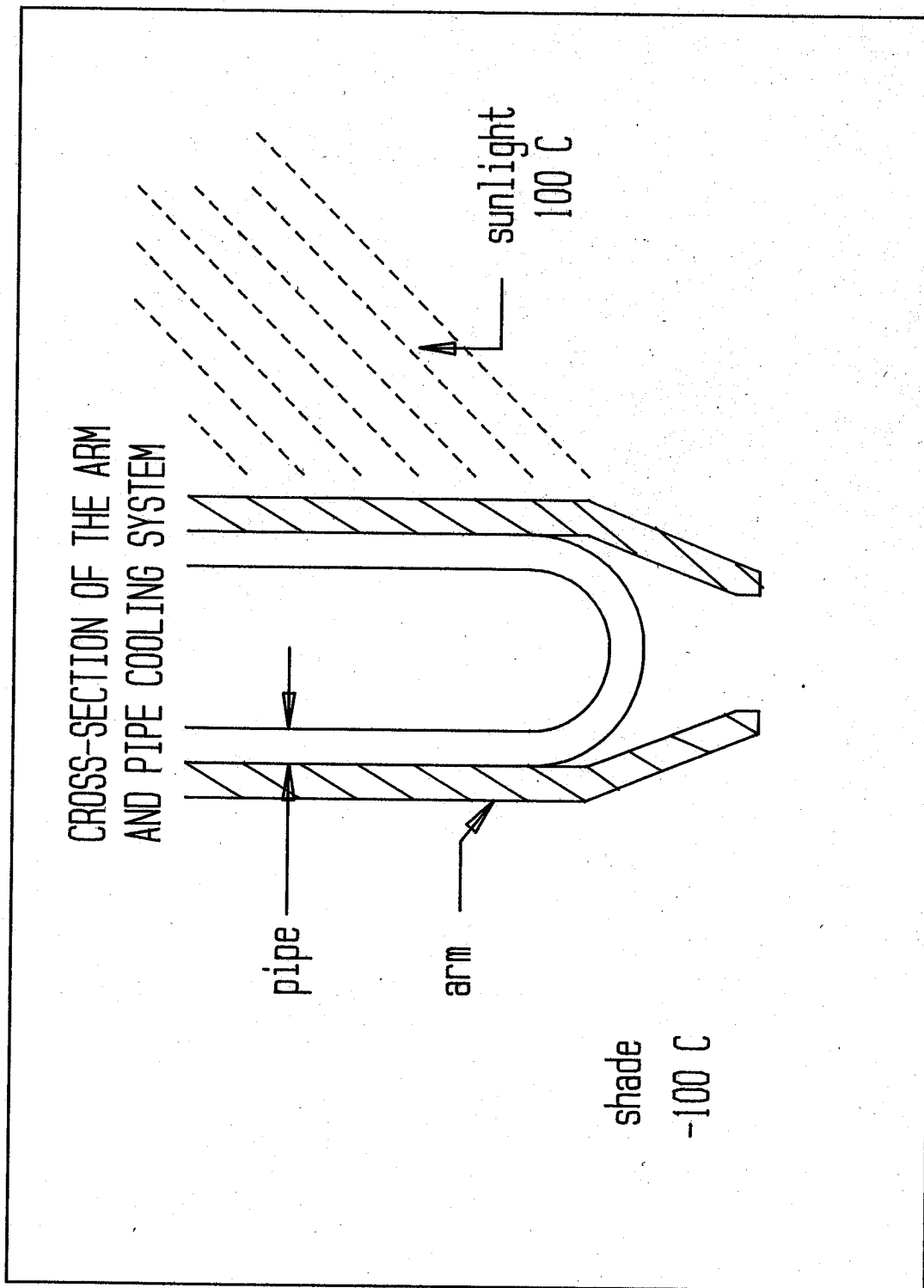


Table 2

Q = 2164.80
 SIGMA = 0.00
 E = 0.80
 Ts = 210.80
 K = 0.14

TEMPERATURE

AREA

360	3.22
370	2.85
380	2.53
390	2.26
400	2.02
410	1.82
420	1.64
430	1.48
440	1.34
450	1.22
460	1.12
470	1.02
480	0.93
490	0.86
500	0.79
510	0.73
520	0.67
530	0.62
540	0.57
550	0.53
560	0.50

ARMTEMP

ABSORPTION

RADIATION

QOUT

366	249.17	996.70	747.52
356	219.81	879.22	659.42
346	192.81	771.24	578.43
336	168.06	672.23	504.18
326	145.42	581.68	436.26
316	124.77	499.08	374.31
306	105.99	423.97	317.98
296	88.97	355.87	266.90
286	73.58	294.33	220.75
276	59.73	238.92	179.19
266	47.31	189.22	141.92
256	36.20	144.82	108.61
246	26.33	105.32	78.99
236	17.59	70.37	52.77
226	9.89	39.58	29.68
216	3.15	12.62	9.46
206	-2.71	-10.85	-8.14
196	-7.78	-31.13	-23.35
186	-12.13	-48.54	-36.40
176	-15.84	-63.35	-47.52
166	-18.96	-75.85	-56.89

ABSORPTION	RADIATION	QOUT	TFLUID
249.17	996.70	747.52	358
219.81	879.22	659.42	349
192.81	771.24	578.43	340
168.06	672.23	504.18	331
145.42	581.68	436.26	322
124.77	499.08	374.31	312
105.99	423.97	317.98	303
88.97	355.87	266.90	293
73.58	294.33	220.75	284
59.73	238.92	179.19	274
47.31	189.22	141.92	265
36.20	144.82	108.61	255
26.33	105.32	78.99	245
17.59	70.37	52.77	235
9.89	39.58	29.68	226
3.15	12.62	9.46	216
-2.71	-10.85	-8.14	206
-7.78	-31.13	-23.35	196
-12.13	-48.54	-36.40	186
-15.84	-63.35	-47.52	176
-18.96	-75.85	-56.89	167

HTABSORP	HTRADIATION	QOUT	HTFLUID
231.26	925.04	693.78	359
261.62	1046.46	784.85	358
294.53	1178.14	883.60	357
330.16	1320.63	990.47	356
368.63	1474.51	1105.88	355
410.09	1640.38	1230.28	353
454.71	1818.83	1364.13	352
502.63	2010.50	1507.88	351
554.01	2216.02	1662.02	349
609.01	2436.04	1827.03	347
667.81	2671.23	2003.42	345
730.57	2922.27	2191.70	344
797.46	3189.85	2392.39	341
868.67	3474.69	2606.02	339
944.38	3777.51	2833.14	337
1024.77	4099.06	3074.30	334
1110.02	4440.09	3330.07	332
1200.34	4801.37	3601.03	329
1295.92	5183.69	3887.77	326
1396.96	5587.85	4190.89	323
1503.67	6014.67	4511.00	320

CANTILEVER BEAM PROGRAM

1 LBL CANT	51 *	101 *
2 END 3	52 +	102 +
3 L?	53 RCL 03	103 6
4 PROMT	54 *	104 /
5 STD 2	55 TCL 03	105 RCL 10
6 E?	56 *	106 /
7 PROMTY	57 TCL 07	107 Y=
8 I?	58 XEQ 04	108 GOTO D
9 PROMPT	59 RCL 07	109 LBL B
10 *	60 3	110 RCL 06
11 STD 10	61 Y^x	111 EQ 04
12 A ?	62 *	112 RCL 06
13 PROMPT	63 FS ? 02	113 2
14 STD 06	64 CLX	114 /
15 P?	65 STD 09	115 RCL 01
16 PROMPT	66 RUN	116 -
17 STD 03	67 RCL 01	117 RCL 03
18 B ?	68 4	118 *
19 PROMPT	69 /	119 RCL 01
20 STD 07	70 RCL 07	120 *
21 W ?	71 -	121 RCL 07
22 PROMPT	72 RCL 01	122 XEQ 04
23 STD 04	73 *	123 3 RDN
24 C?	74 RCL 07	124 RCL 01
25 PROMPT	75 X^2	125 6
26 STD 08	76 1.5	126 /
27 M?	77 *	127 RCL 01
28 PROMPT	78 +	128 2
29 STD 05	79 RCL 01	129 /
30 LBL E	80 X^2	130 -
31 X?	81 *	131 RCL 01
32 PROMPTJ	82 RCL 09	132 *
33 STD 00	83 +	133 RCL 07
34 STOP	84 RCL 04	134 X ^2
35 LBL A	85 6	135 2
36 RCL 06	86 *	136 /
37 XEQ 04	87 RCL 01	137 +
38 LASTX	88 3	138 RCL 04
39 *	89 XLS Y	139 *
40 CHS	90 FS ? 02	140 *
41 3	91 CLX	141 -
42 *	92 +	142 RCL 08
43 FS?02	93 RCL 05	143 XEQ 04
44 0	94 *	144 RDN
45 RCL 01	95 RCL 01	145 2
46 RCL 06	96 /	146 RCL 05
47 3	97 Y=	147 RCL 01
48 *	98 RCL 05	148 A VIEW
49 -	99 *	149 STOP
50 TCL 01	100 RCL 01	150 END

APPENDIX 5

PERFORMER

PERFORMANCE

In calculating a digging speed, several assumptions were made. First we assumed two different vertical speeds. The speed at which the digger dropped is .5 m/s and the speed it lifted was .25 m/s. Next we assumed a rotation speed of 7.5 rev/min. We assumed that the bucket emptied the load 90 degrees from the point where it was filled. The bucket is working with a 1 m vertical lift. We allowed a time period of 2 s for digging and 2 s for unloading. The volume of one bucket is .5 cubic meters. Therefore, we have:

$$\text{Volume of one lift} = 2(.5) = 1 \text{ cubic meter}$$

$$\begin{aligned}\text{Speed of rotation} &= (7.5 \text{ rev/min})(360 \text{ deg/rev})(1 \text{ m/60 s}) \\ &= 45 \text{ deg/s}\end{aligned}$$

Times:

$$\text{Drop} = 1 \text{ m} / .5 \text{ m/s} = 2 \text{ s}$$

$$\text{Lift} = 1 \text{ m} / .25 \text{ m/s} = 4 \text{ s}$$

$$\text{Rotation} = 2 \text{ swings } (90 \text{ deg/swing} / 45 \text{ deg/s}) = 4 \text{ s}$$

$$\text{Digging time} = 2 \text{ s}$$

$$\text{Unloading time} = 2 \text{ s}$$

$$\text{Total time} = 14 \text{ s /cubic meter}$$

So the digger digs at a rate of 260 cubic meters/hr. At this rate the digger could dig a ditch 1 km long by 1 square meter in 4 hours.

APPENDIX 6

INTERFACE PIN CONNECTION

ANALYSIS OF PIN CONNECTION

First, the tensile preload and the fluctuating tensile load was calculated, which was found to be 450 N and 0 to 7200 N, respectively. Titanium alloy ASTM B265, Grade 5 (6% Al, 4% vanadium) is used with tensile strength of 900 Mpa and a yield strength of 830 Mpa. So,

$$S'_e = .5S_{ut} = .5(900 \text{ Mpa}) = 450 \text{ Mpa}$$

The diameter is designed for infinite life, with geometric stress-concentration factor of 4, safety factor of 3, ground finished, and 95% reliability.

The following equations were used to calculate the minimum diameter of the pin.

$$S_e = K_a K_b K_c K_d K_e S'_e$$

$$K_a = .9 \quad (\text{ground finished})$$

$$K_b = .869(.5)E^{-.097} = .93 \quad (.3 < d < 10 \text{ in})$$

$$K_c = .87 \quad (\text{Reliability of 95\%})$$

$$K_d = 1 \quad (T \leq 840 \text{ F})$$

$$K_e = 1/k_f = 1/4 = .25$$

These are all the necessary corrections, so that

$$S_e = (.9)(.93)(.87)(1)(.25)(450 \text{ Mpa}) = 82 \text{ Mpa}$$

Next we determined the stresses in terms of their dimensions. The static stress is

$$\sigma_s = F_s/A = F_s/(\pi \times d^2)/4 = 880 \text{ Kpa}$$

The stress range is

$$\sigma_r = F_r/A = F_r/(\pi \times d^2)/4 = 14 \text{ Mpa}$$

Then,

$$\sigma_m = \sigma_s + \sigma_a = 880/d^2 \text{ Kpa} + 7/d^2 \text{ Mpa} = 700 \text{ Mpa}$$

Therefore,

$$\sigma_a/\sigma_m = .89$$

To relate the stresses and strengths, a fatigue diagram is plotted. Note that only the tensile side is needed. The intersection of the modified Goodman line with another line at a slope of $\sigma_a/\sigma_m = .89$ defines two values of strength corresponding to the stress σ_a , and S_m is a strength corresponding to the stress σ_m .

For the safety factor of 3

$$\sigma_a \leq S_a / 3$$

From the fatigue diagram

$$7/d^2 = 72/3 \quad d \geq 15 \text{ mm}$$

We therefore choose $d = 15 \text{ mm}$.

Fatigue Diagram for Interface Pin Connection

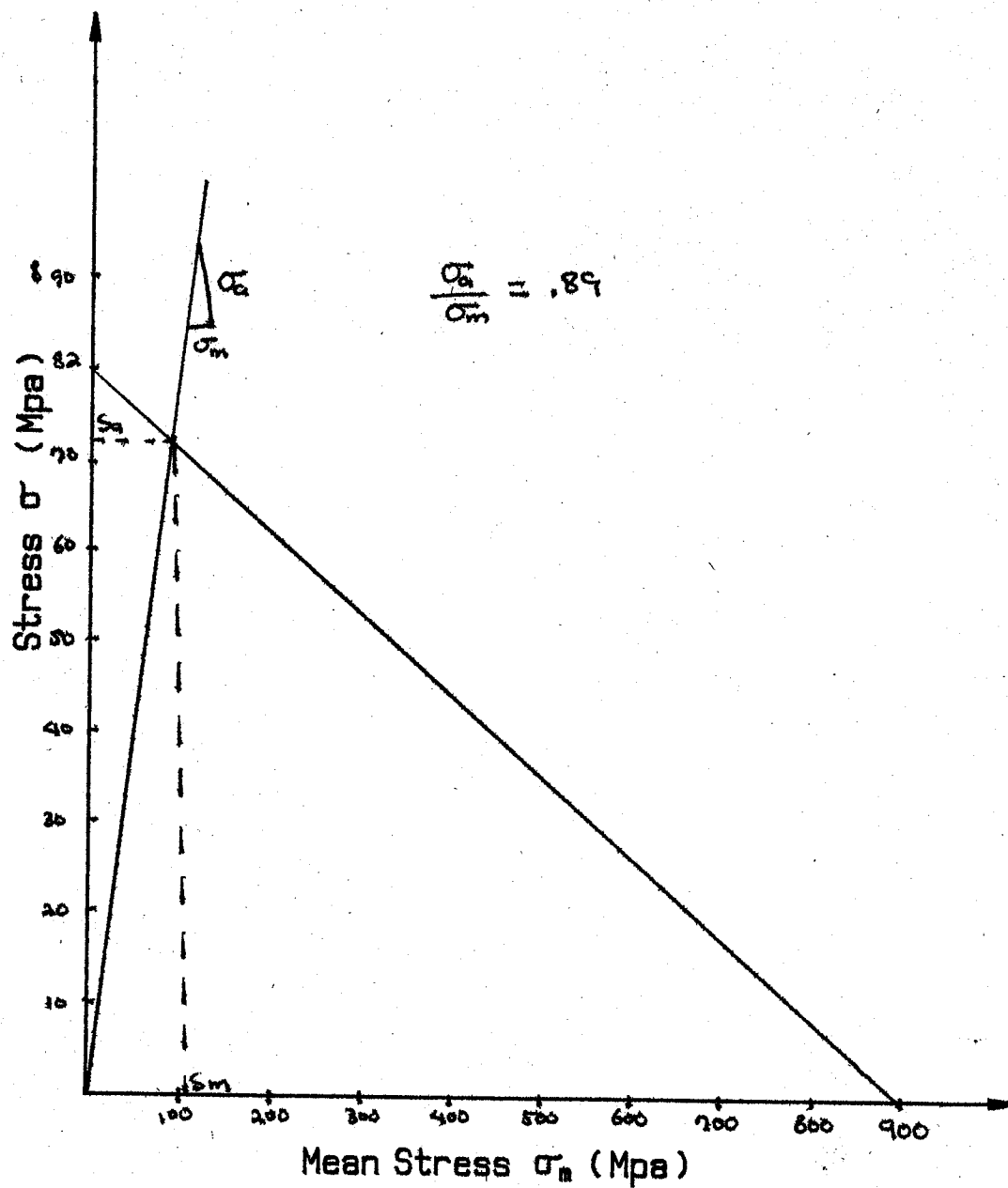
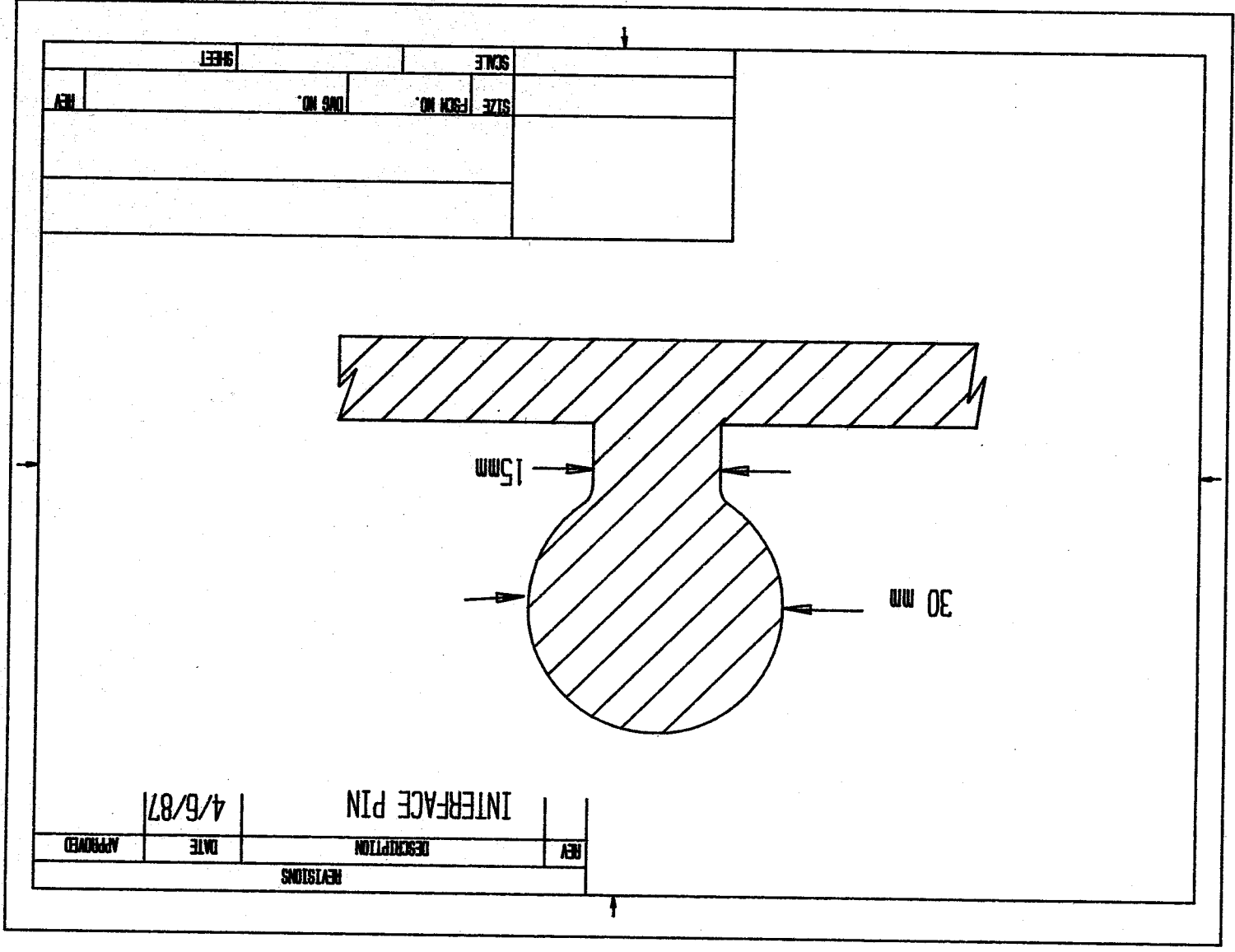
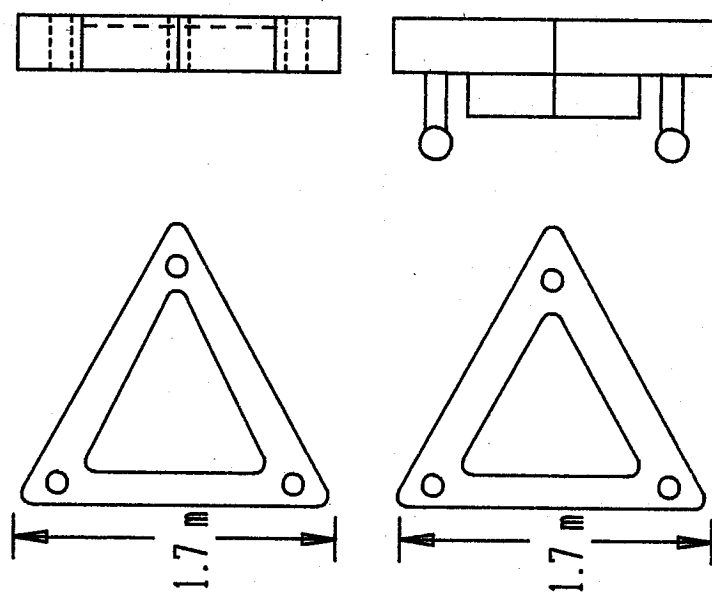


Figure 6-1



INTERFACE PIN CONNECTION



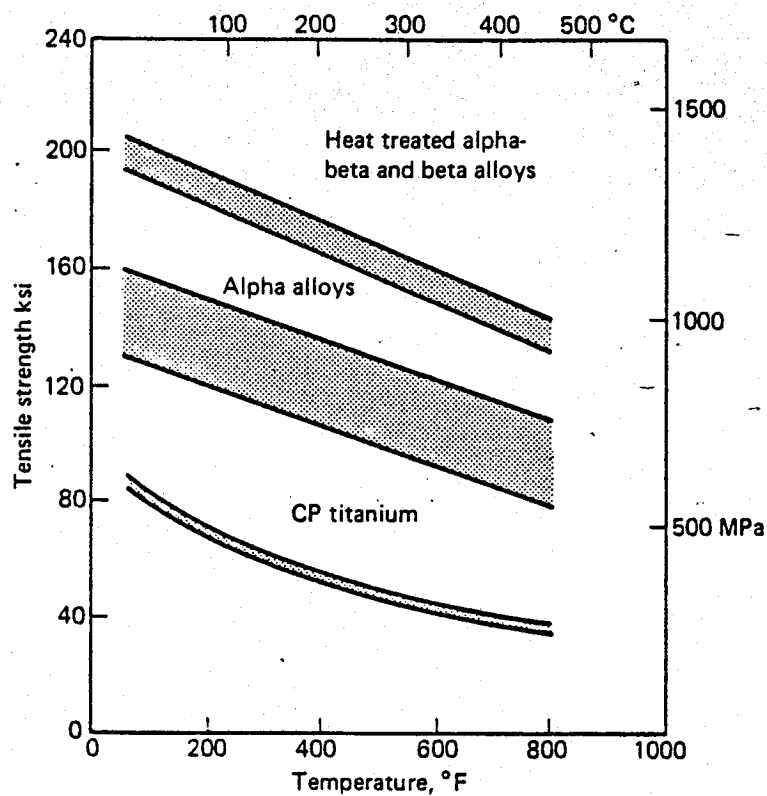
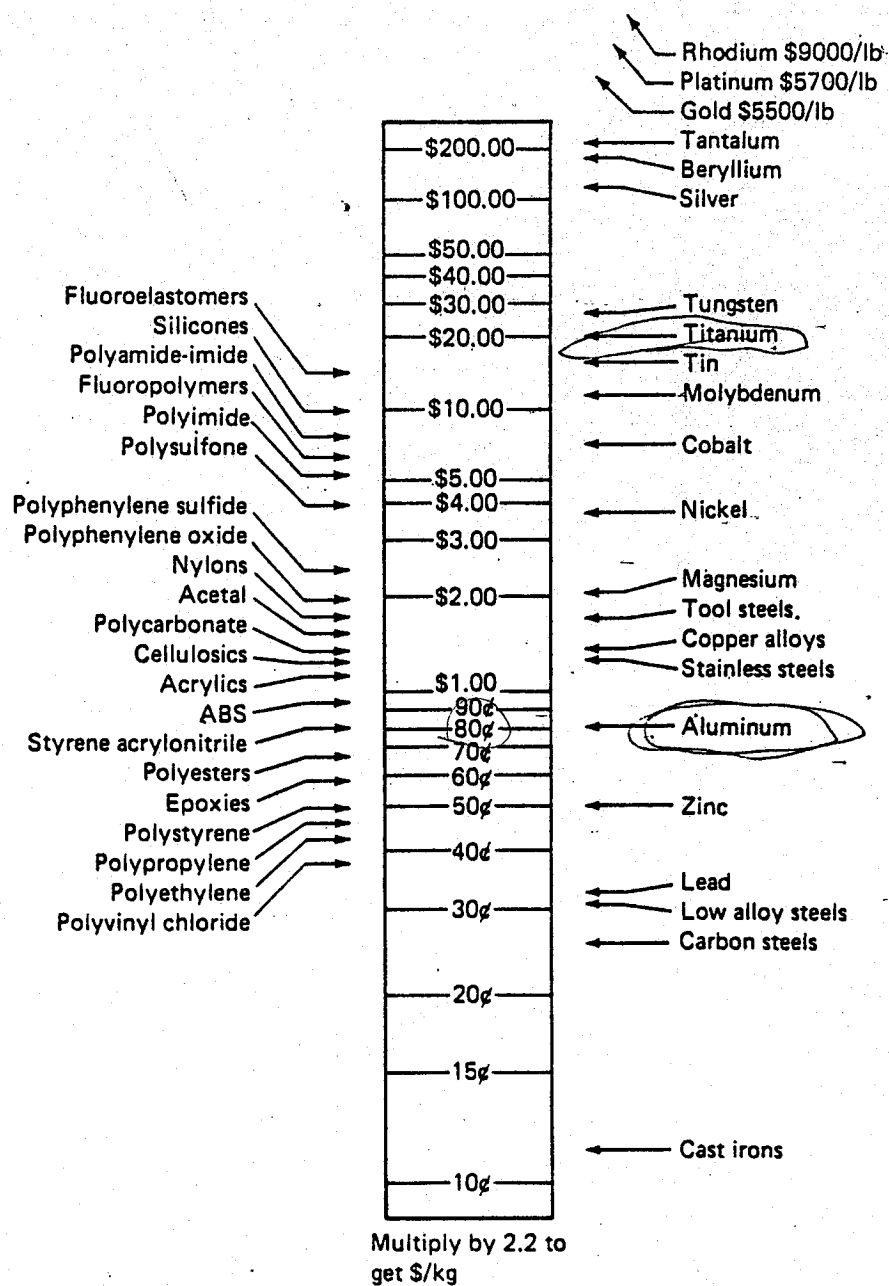
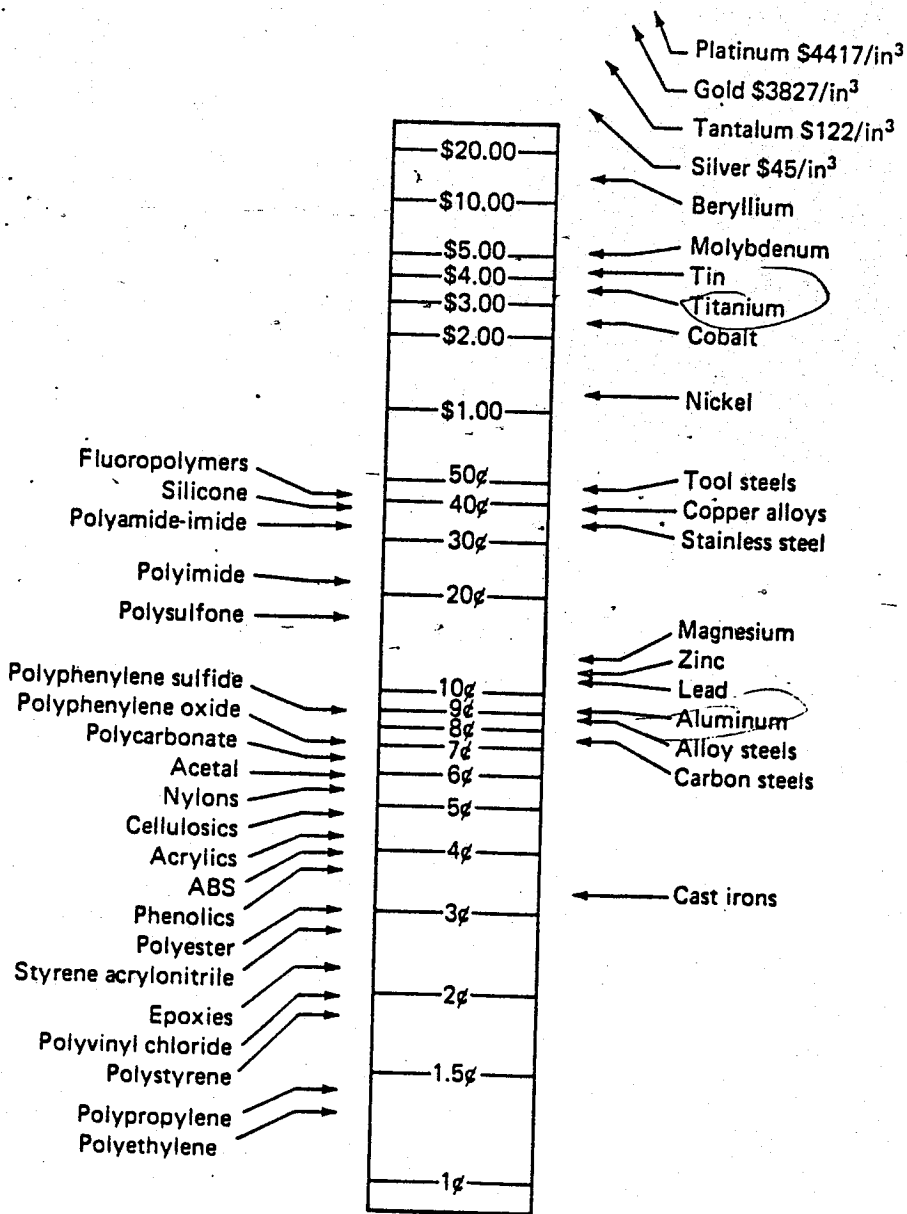


Figure 16-5 Tensile strength of titanium alloys at elevated temperatures

* Engineering Materials
Properties and selection 2nd edition
 by Kenneth Budinski



*Figure 19-3 Comparative costs of engineering materials per pound. Plastics are in molding resin form; metals are in the form of mill products.



Divide by 16.4 to
convert to \$/cm³

* Figure 19-4 Cost of some engineering materials per cubic inch

* Table 20-1 Fracture Toughness of Various Engineering Materials

		CRITICAL STRESS INTENSITY FACTORS	
MATERIAL		ksi $\sqrt{\text{in}}$	MN m ^{-3/2}
Metals	Pure ductile metals (Cu, Ni, Ag, etc.)	90-320	100-350
	HY 130 steel	155-160	170-175
	Low-carbon steel	110-127	120-140
	18% Ni maraging steels	75-100	75-100
	PH stainless steels	60-130	66-143
	Titanium alloys	32-98	35-108
	4340 steel	40-86	44-78
	Medium-carbon steel	36-46	40-50
	Aluminum alloys	20-45	22-50
	Gray cast iron	5-18	6-20
	Cemented carbides	13-15	14-16
Plastics	Beryllium	3-5	4
	Glass-reinforced epoxy (RTP)	38-55	42-60
	ABS	2.7-3.6	3-4
	Polypropylene, nylon	2.7	3
	High-density polyethylene	1.8	2
	Polystyrene	1.8	2
Ceramics	Polycarbonate	0.9-2.4	1-2.6
	Aluminum oxide Al ₂ O ₃	2.7-4.5	3-5
	Silicon nitride Si ₃ N ₄	3.6-4.5	4-5
	Silicon carbide SiN	2.7	3
	Magnesium oxide MgO	2.7	3
	Soda lime glass	0.6-0.7	0.7-0.8

APPENDIX 7

JOINTS

Appendix 7

In choosing the size of the pins for the digger, two types of loading are considered. First, the impact loading is the force applied to the pin joints when the digger hits a rock and reverse the force back through the digger. Next, there is a static load on the joints due to the weight of the digger held at a static equilibrium position.

Impact Load

For a solid circular beam,

$$T = 4V/3A$$

where,

T = Ultimate Tensile Strength = 690 kN/meter square

V = Shear force

A = Cross sectional area of beam

This equation can be rewritten as

$$r = (4VN/3\pi T)^{.5}$$

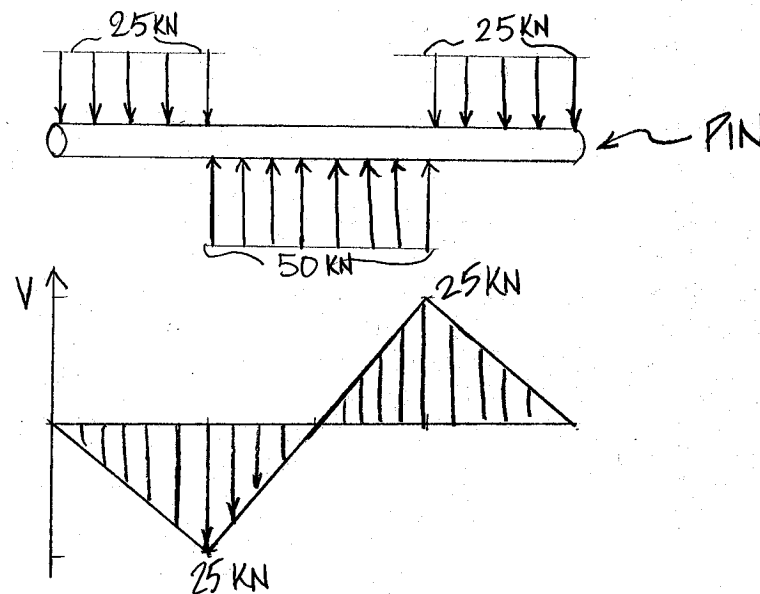
where,

r = the radius of the beam

N = safety factor, 2

The Ultimate Tensile Strength for Ti-13V-11Cr-3Al in the uniaxial direction is 1,380,000 kN/m². Therefore, the maximum shear stress will be half of this, which is 690,000 kN/m².

example:



$$V = 25 \text{ kN}$$

$$r = (4 * 25 * 2 / (690,000 * 3 * \pi))$$

$$r = .55 \text{ cm}$$

Static Load The equation to find the radius of the pin for static loading will be the same as that of the impact loading. The only difference is, instead of using the Ultimate tensile strength, we are using the yield strength of 630,000 kN/m².

TO FIND THE RADIUS OF PINS AT JOINTS

$$\tau = 4 \cdot V \cdot N / \text{shear} \cdot 3 \cdot \pi \cdot I$$

SAFETY FACTOR OF 2

STATIC
LOAD

$$\tau_{\max} = 630,000 \text{ KN/m}^2$$

PIN #	SHEAR FORCE (KN)	RADIUS (CM)	(IN)
1	0.25	0.06	0.02
2	0.3	0.06	0.03
3	0.55	0.09	0.03
4	0.55	0.09	0.03
5	0.3	0.06	0.03

IMPACT
LOAD

$$\tau_{\max} = 690,000 \text{ KN/m}^2$$

PIN #	SHEAR FORCE (KN)	RADIUS (CM)	(IN)
1	10	0.35	0.14
2	3	0.19	0.08
3	25	0.55	0.22
4	75	0.96	0.38
5	8.5	0.32	0.13

Lowest

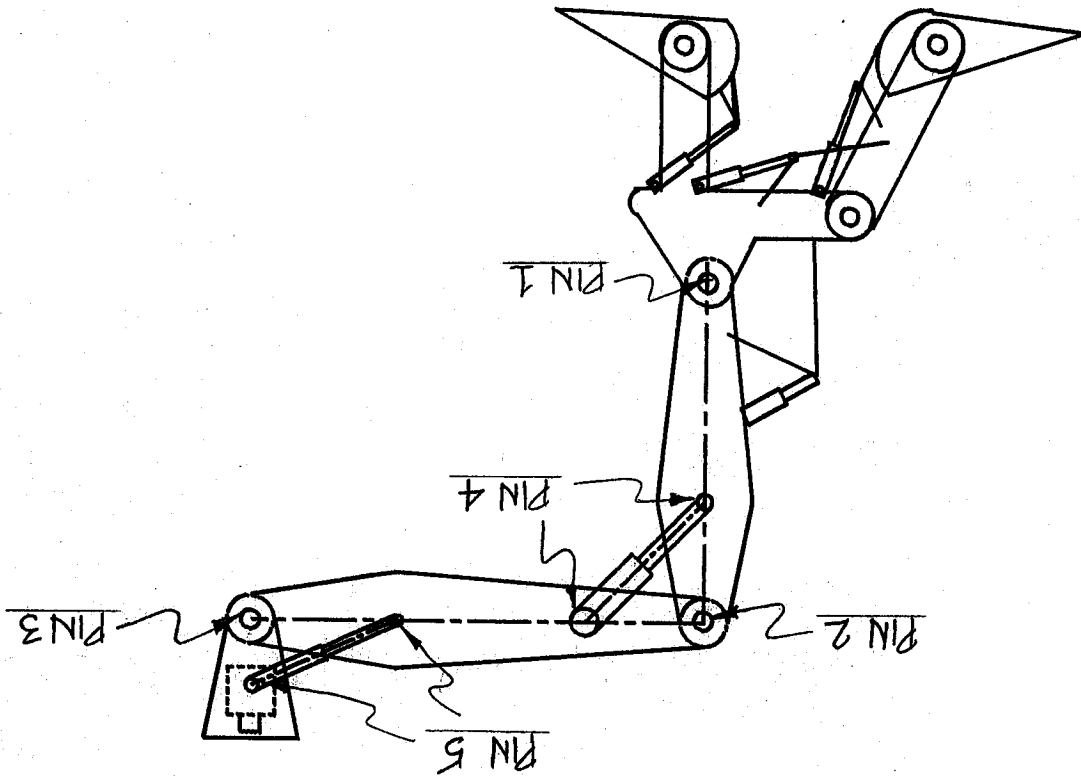


FIGURE 7-1

Table B-10 Tensile Properties of Solution Treated and Aged 13V-11Cr-3Al Titanium Alloy at Cryogenic Temperatures

Temperature (°F)	^{In impact} Ultimate Strength (ksi)	^{by static} Yield Strength 0.2% Offset (ksi)	Elongation, in 2-in. (%)	Modulus of Elongation (psi x 10 ⁶)	Weld Strength (ksi)
70	206.0 197.2 <u>195.2</u> 199.5 avg	-- 184.3 <u>181.3</u> 182.8 avg of 2	5.5 7.0 <u>7.0</u> 6.5 avg	16.1	143.8 143.5 <u>145.9</u> 144.4 avg
-320	218.0 185.0 <u>201.0</u>	-- -- --	--* --* --†	16.8	125.6 (95.7) <u>129.8</u> 127.7 avg of 2
-423	--	--	--	--	81.3 88.3 (49.5) 84.8 avg of 2
*Failed through pinhole.					
†Failed outside gage mark.					

Martin-CR-64-74

BEARING LOCATIONS

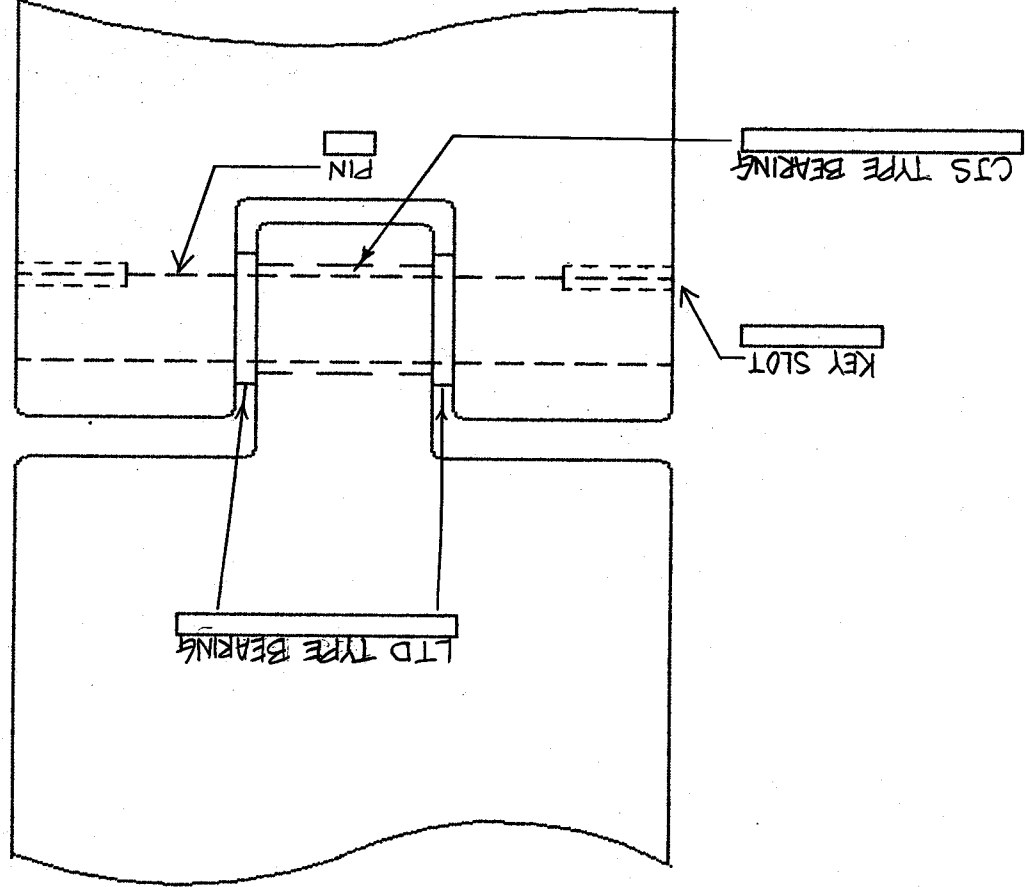


FIGURE 7-2

Fiberglide®

SELF-LUBRICATING BEARINGS

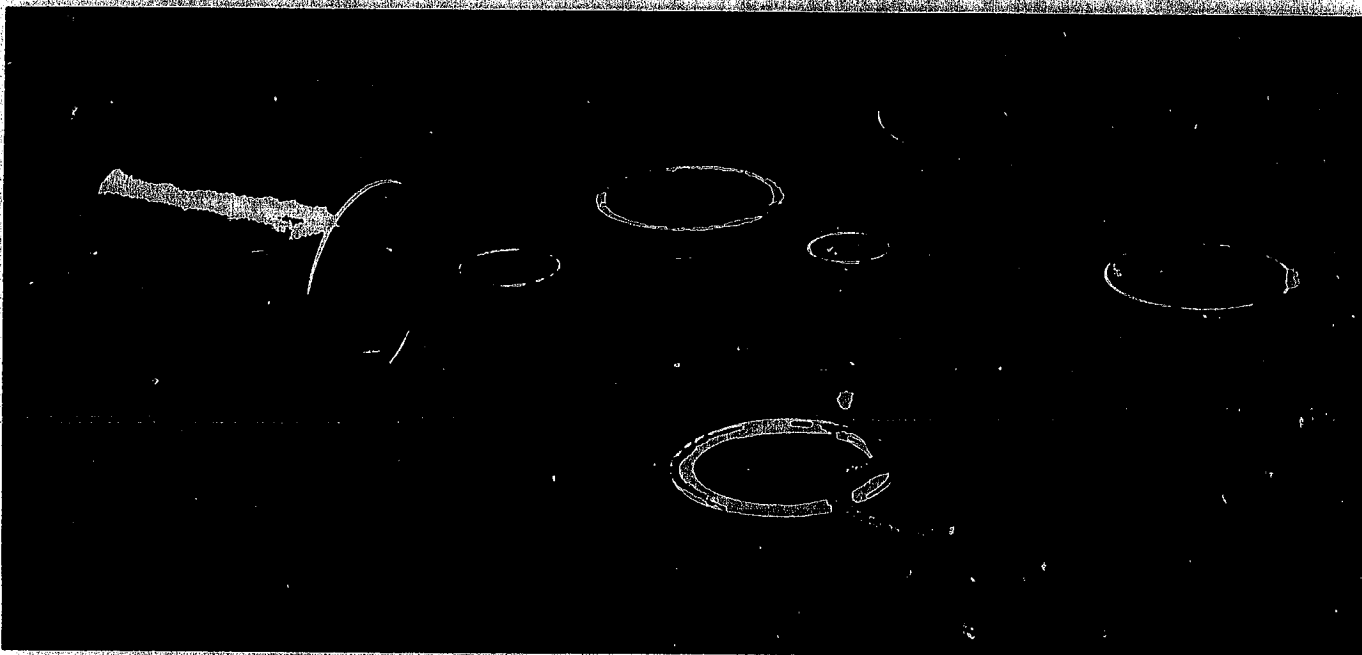
"FIBERGLIDE®" is a proprietary self-lubricating bearing material of woven Teflon® (polytetrafluoroethylene or PTFE) fibers applied to a rigid backing. To assure the best possible bond between PTFE fibers and backing material, a secondary, more readily bondable fiber (which may vary with application requirements) is interwoven with the PTFE fibers so that Teflon® is predominantly presented on the bearing side of the fabric.

FIBERGLIDE® bearings are unique in their ability to resist Teflon® cold-flow under extremely high loads because the monofilament fibers have a tensile strength approximately 15 times greater than straight PTFE resins.

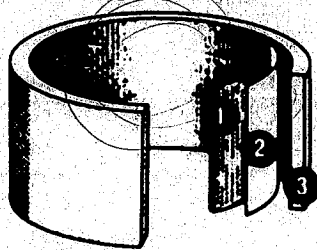
Cold flow is also minimized by the effective entrapment of the fiber bundles by the high-strength bonding resins.

FIBERGLIDE® bearings are completely self-lubricating and normally run dry. However, they can also be used where lubricating or other fluids are present. Operating dry, FIBERGLIDE® bearings are recommended where low surface speeds are combined with high loads.

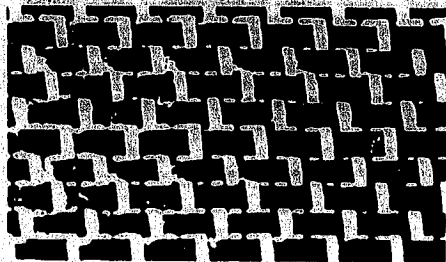
FIBERGLIDE® bearings are available with many backing materials in a wide variety of standard configurations. In addition, LSI/Transport Dynamics offers special bearings with an almost unlimited range of configurations and metal backings.



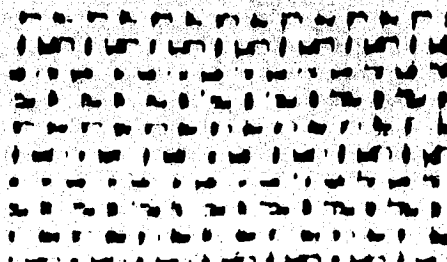
Teflon® is a registered trademark of E.I. DuPont de Nemours & Co.



Construction of typical FIBERGLIDE® bearing
(1) PTFE fabric
(2) Adhesive bonding agent
(3) Metal or molded phenolic backing



Under the microscope, the bearing side (showing dark) of FIBERGLIDE® liner presents mainly PTFE fibers



Secondary and more readily bondable fiber (showing white) is interwoven with the PTFE as illustrated in this microphoto of the bonding side

Here are 15 reasons why you should be using Fiberglide® Bearings instead of conventional lubricated types.

1. Operation without lubrication while tolerating many lubricating and non-lubricating fluids.
2. High load-carrying capacity (up to 20,000 psi)
3. Low coefficient of friction (down to 0.02)
4. Freedom from stick-slip.
5. Absence of cold-flow tendencies of solid and filled PTFE resins
6. High resistance to fatigue under shock loads
7. Resistant to attack by most substances
8. Eliminates fretting corrosion
9. Operation at temperatures beyond the range of most lubricants (- 320 to + 420F)
10. High wear resistance
11. Inherent dampening qualities
12. Good dimensional stability
13. Wide range of mating materials acceptable
14. Electrically non-conducting
15. Non-magnetic

Fiberglide®

BEARINGS—OPERATING PARAMETERS

Many factors affect the overall performance of FIBERGLIDE® bearings. Those of primary concern include applied load, surface velocity, operating mode, surface temperature, mating surface finish and running clearance. All performance values referred to in this section are based on dry operation. When running in a fluid atmosphere, FIBERGLIDE® bearings may have reduced limitations and performance. Where application requirements exceed those shown, consult LSI/Transport Dynamics engineering department for specific recommendations.

Fiberglide® lined bearings are designed to be used under oscillating motion, interrupted start-stop, or axial motion. They are recommended where high loads are combined with low surface speeds, rather than low load high RPM type application.

DESIGN CALCULATIONS (journals-oscillating motion)

$$\text{Proj. Area (IN}^2\text{)} = \text{SHAFT DIA MAX (OR NOM. I.D.)} \times \text{LENGTH}$$

$$\text{P PRESSURE (PSI)} = \text{LOAD (LBS)} \div \text{Proj. Area}$$

$$\text{V. Velocity (FPM)} = \frac{\text{Shaft Dia Max} \times \pi}{12} \times \frac{4 \times \text{Osc. Angle}^\circ \times \text{CPM}}{360}$$

Bearing Wear

As indicated above, bearing wear is affected by many factors. For the most part, tests conducted by Transport Dynamics subject journal bearings to high (10,000 psi) loads with the bearing fixed and the shaft oscillating. The values shown in the chart on page 8 are representative of the normal wear rate range that can be expected when amplitude is $\pm 45^\circ$, frequency is 10 CPM, and shaft finish is 16 RMS under room temperature conditions.

It will be noted that a wear-in period takes place during the first few thousand cycles. During this period some PTFE is transferred to the mating surface. In addition, the fibers are generally reoriented, the high spots of the weave are flattened and adjacent fibers tend to blend together. After the break-in period, the bearing surface will become smooth and shiny.

Because of the many variables which influence wear, it is extremely difficult to project bearing life for all types of applications. For this reason, the Transport Dynamics engineering department should be consulted when questions of this nature arise.

Bearing Load Limits

Static Pressure Limit (constant pressure*)

10,000 psi with phenolic backing

20,000 psi with steel backing

*Where repeated impact loading is applied, these values should be reduced to meet fatigue life requirements.

Dynamic Pressure Limit

2,000 to 4,000 psi for best life

10,000 psi suggested minimum

Velocity Limit

Under dry running conditions, the maximum allowable surface velocity will depend on the applied load and other operating parameters. In general, surface speed should be kept below 35 FPM.

PV Factor

For plain, dry-running bearings, it is often helpful to reference a pressure-velocity (PV) factor as a guide in determining bearing capability. It should be understood that this factor is actually a variable which reflects the point where surface temperatures are at a maximum, but are still stable. The maximum PV established for FIBERGLIDE® is:

PV continuous—10,000

PV Maximum—20,000

Temperature Limit

Normal operating temperatures should be kept below 200F for standard Fiberglide® bearings. An increase in wear rates may be experienced at temperatures above 150F. Note that at elevated operating temperatures, the PV limit will be decreased in order to prevent the surface temperature from exceeding 200F. (environmental temperature plus friction heat generated). When temperatures exceed 200F or fall below -200F, consult Transport Dynamics engineering department for specific recommendations.

Coefficient of Expansion

When bonded to a metal backing, FIBERGLIDE's coefficient of expansion can normally be regarded as identical to that of the backing, with steel backing 8.4×10^{-6} IN/IN/°F, with laminated phenolic backing approx. 17.0×10^{-6} IN/IN/°F.

A COMPARISON OF FIBERGLIDE® WITH OTHER SELF-LUBRICATING TYPES

	METAL-BACKED FIBERGLIDE®	FILLED PTFE	NYLON	POROUS BRONZE
MAX. STATIC LOAD PSI	20 000	2 500	1 000	8 500
MAXIMUM PV VALUE	20 000	10 000	3 000	50 000
TEMPERATURE RANGE, F	400 -200	400 -500	65 -200	65 -250
MAXIMUM SPEED FPM	35	100	50	1 200
CHEMICAL RESISTANCE	GOOD	EXCELLENT	FAIR	FAIR
MINIMUM COEF. OF FRICTION	.02	.02	.25	.05
TYP. DYNAMIC LOAD (P.S.I.)	2 000 TO 10 000			

Coefficient of Friction

Coefficient of friction depends upon type of movement, finish of mating surface, ambient temperature, bearing pressure, velocity and other variables. Figs. 1, 2 and 3 were obtained from flat specimens and may be used as a guide. Note in Fig. 1 that the coefficient drops off as bearing load increases. This offers the advantage of using the smallest bearing sizes to obtain the least amount of friction. Fig. 2 shows the coefficient of friction increasing as surface velocity increases from 0-20 FPM. This feature is particularly desirable for vehicle steering systems.

$$10,000 \text{ psi} = 69,000 \text{ KN/m}^2$$

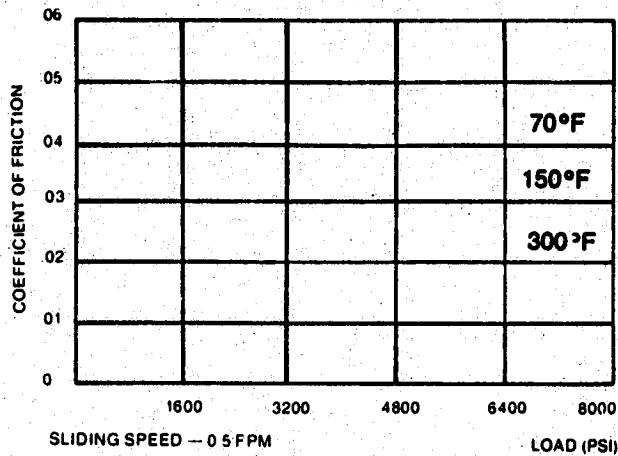
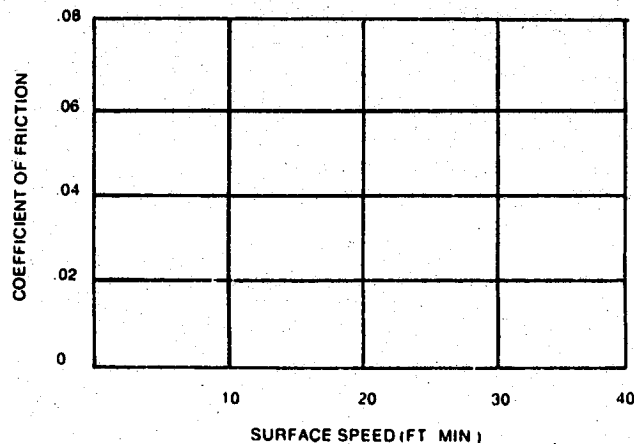
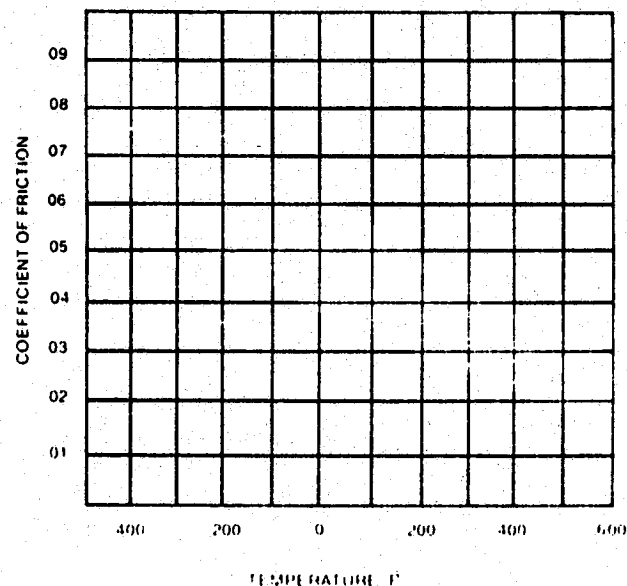
Fig 1 — Effect of load and temperature on Fiberglide[®] bearing frictionFig 2 — Coefficient of friction at 10,000 psi.
Normal unit load and 70 F vs surface speed

Fig 3 — Effect of temperature on coefficient of friction

MATING SURFACES

FIBERGLIDE[®], being NON-METALLIC, will operate against most metals, but better performance is usually obtained with the hardest available mating surfaces. Hardened steel, hard anodized aluminum, hard chrome or nickel plate are recommended. A surface hardness of 45-50 Rc is desirable, but satisfactory performance can also be obtained with softer materials. However, the harder the surface, the less likely that it will be nicked or scratched prior to assembly. Generally, a surface finish on the mating components of 16-32 micro-inch should be provided. Shaft materials or surface treatments should be selected that will effectively resist corrosion. The influence of different surface hardness and surface finish is shown below.

To determine the approximate reduction in life for different values of shaft finish and hardness, see below.

SURFACE FINISH Micro-Inches	LIFE FACTOR	HARDNESS Rockwell Reading	LIFE FACTOR
8-16	1.00	Rc 50	1.00
32	0.55	Rc 40	0.60
63	0.20	Rc 30	0.40

Dirty Environments

FIBERGLIDE[®] can tolerate small amounts of dirt, but reduced bearing life will result. Optimum life is achieved if dirt or abrasive particles are excluded. If a dirty environment is likely, we recommend installation of a simple seal.

Running Clearance

As a general rule, close running fits, and often slight interference fits (.0005 in.), are selected for oscillating motion when minimum starting torque is less important than the elimination of free play. For constant rotation, a free-running fit is normally recommended, the exact amount depending on bearing bore size. A rule of thumb would be 0.0015 in. per inch of bore (bearing installed).

Bearing Housing Fits

FIBERGLIDE[®] journal bearings (CJS/CJT type) are installed into the housing bore using a press fit. Recommended housing bores should be held to the tolerance shown to insure the proper press fit. After installation, the journal bore will then fit the shaft properly, i.e., with optimum clearance for longest life.

The LJS type bearing is hand slip fit into its recommended housing bore to provide optimum fit-up.

Contaminating Fluids

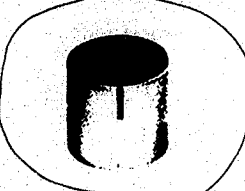




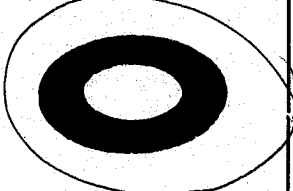
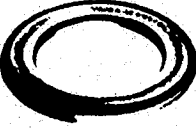
FIBERGLIDE[®] can tolerate most fluids or contaminants found in bearing applications. Although some reduction from dry bearing life will result, following are some of the environments in which these bearings have operated successfully:

Hydraulic oils	Mild acids
Greases	Ammonium hydroxide
Gasoline	Lubricating oils
Kerosene	Detergent solutions
Toluene	Seawater
	Liquid Nitrogen

Fiberglide®

SELF-LUBRICATING BEARINGS

SELECTION GUIDE

TYPE	DESCRIPTION	DIMENSIONS*	APPLICATIONS
	CJS Journal bearings, coiled steel backing, zinc plated.	Nom. shaft diam.: .375 to 10.000 Bearing length: .250 to 6.50 Wall thickness: .045 to .093	Ideal for automotive vehicles, farm equipment, textile and woodworking machinery. Has plated carbon steel backing, other metals available.
	CJT Journal bearings, thin-walled, coiled steel backing, zinc plated.	Nom. shaft diam.: .500 to 10.000 Bearing length: .375 to 6.50 Wall thickness: .060	A lighter walled bearing for direct replacement of conventional bushings of the same size. Applications similar to CJS above.
	CJM METRIC Journal bearings, coiled steel backing, zinc plated.	Nom. shaft diam.: 8MM to 120MM Bearing length: 8MM to 165MM Wall thickness: 1.0 to 2.4 MM	Application similar to CJS above, but manufactured to metric dimensions.
	LJS Journal bearings, liner type. Non-metallic.	Nom. shaft diam.: 1.000 to 12.000 Length: .375 to 6.50 Wall thickness: .022 to .062	As a thin-walled sleeve, this bearing may be used in butterfly valves, <u>trunnion bearings</u> , valve stem bushings, food handling machinery.
	FTS Thrust bearings, metal-backed, single sided.	Nom. shaft diam.: .250 to 3.250 I.D.: .280 to 3.312 O.D.: .500 to 4.875 Thickness: .030 to .060	Typical applications include kingpin assemblies, industrial valves and valve actuators. Zinc plated mild steel is used as a backing material.
	LTD Thrust bearings, laminated phenolic-backed, double sided.	Nom. shaft diam.: .250 to 3.250 I.D.: .280 to 3.312 O.D.: .500 to 4.875 Thickness: .030 to .094	Applications similar to FTS above but also include wet or corrosive atmospheres. LTD washers use Fiberglide on both sides to maximize bearing life. Non-metallic.
	FTP Thrust packs. Two piece assembly.	I.D.: 1.000 to 3.000 O.D.: 1.750 to 4.625 Thickness: .130	These packs are ideal for vehicle kingpin assemblies, frame hinges. Includes a self-contained dust seal and hard plated wear surface.

*All dimensions are in inches except for CJM series. In addition to the standard size ranges listed, all Fiberglide® bearings can be supplied in larger diameters and special configurations. Inquiries should be directed to the Sales Dept.

FIBERGLIDE® self-lubricating bearings are manufactured on a per order basis for OEM requirements. Overruns from these orders are often available from factory stock.

APPENDIX 8

PROGRESS REPORT

TO: MR. J. W. BRAZELL
FROM: LUNAR DIGGER GROUP -
MARSHALL ALLEN, CHIH-YU CHU, JON COLEMAN, JAE N. LIM,
PAUL THOMAS, BERTRAN WHEATLEY
SUBJECT: WEEKLY PROGRESS REPORT ON THE LUNAR DIGGER

The greatest part of this week was spent preparing for the midterm presentation; however, we also made progress in the following areas:

POWER SUPPLY:

The hydrogen/oxygen fuel cells are being considered. They consist of fuel, an oxidant, and two electrodes in contact with an electrolyte. There are other fuel cells with different fuels and oxidants, some of which use an alkaline electrolyte, but the hydrogen/oxygen combination appears to be the most efficient at this stage of technology. As compared to batteries, fuel cells have a higher energy density when power is needed over an extended period of time, it can also be refilled by resupplying fuel and oxidants. The fuel cells of the Space Shuttle can be used as a design guide. They have an energy density of .15 kw/kg. With the digger needing an estimated 12 hp power source, the fuel cells will have an approximated mass of 60 kg plus the mass of the fuel.

HEAT EXCHANGER

Due to the lack of atmosphere, heat loss from convection to the atmosphere is negligible. The heat generated from the digger must be released by radiation or a heat exchanger.

At first a heat exchanger concept utilizing a solid adsorbent to store the heat was visualized. Zeolite was considered as a form of solid adsorbent. Books on the subject could not be found in the library. An interview with Dr. Shelton was conducted on the subject of heat exchangers. Dr. Shelton could not think of any method of solid adsorbent heat exchanger for space applications. He mentioned solar radiators as a viable means of expelling waste heat. He said Dr. Colwell was working on a NASA space radiator. Dr. Shelton also said that a Brayton steam cycle could use excess heat to produce power. The problem with this concept is that the waste heat would have to be radiated at a lower temperature which means a larger area for the space radiator.

Dr. Colwell explained the basic concepts needed to make a rough design of a space radiator. He said they are found currently on every type of space vehicle. A space radiator is usually made of aluminum with a coating that gives an emissivity of .8. Coatings are available which also give an

absorptivity of .2. A thin sheet of aluminum has aluminum piping welded or brazed to it in a sandwich matter. An aluminum block can have tracks machined into one block and then welded to another block. The second method is more efficient. Basic black body radiation equations are used in analysis. Segmented panels of space radiators can be made for cooling different fluids. Panels can be lightweight and relatively friendly. Never point at sun. Temperature of open space can be assumed to be -BOF for calculation purposes. The higher the temperature of the fluid the faster the heat is radiated and the smaller the area. Dr. Colwell suggested a Rankine steam cycle for power generation, but space radiator area causes some problems. No easy way of sizing a Rankine cycle is known by Dr. Colwell.

Individual efforts:

MARSHALL ALLEN:

- Attended lecture at Fernbank Science Center
- Obtained working knowledge of CADAM system
- Made CAD drawings of hydraulic system components

CHIH-YU CHU:

- Extensive research on use of fuel cells
- Wrote problem statement and objective for the midterm report

JON COLEMAN:

- Produced drawings of the digger using the CADAM system
- Wrote problem statement and objective for the midterm report

JAE N. LIM:

- Produced the outline for the midterm report
- Introduced to CAD system in C. E. building

PAUL THOMAS:

- Prepared speech for the midterm presentation
- Prepared visuals for the midterm presentation

BERTRAN WHEATLEY:

- Extensive research on the heat exchangers
- Discussions with Drs. Shelton and Colwell

**ME 4182
LUNAR DIGGER GROUP
PROGRESS REPORT #3
APRIL 24, 1967**

GROUP MEMBERS: MARSHALL ALLEN, CHIH-YU CHU, JON COLEMAN,
JAE N. LIM, PAUL THOMAS, BERTRAN WHEATLY.

Each member of our group is researching some background information as follows:

INDUCTION MOTORS:

Induction motors are most common in general industrial uses. They are available in sizes of less than 1KW to 1000KW. Rotor resistance is relatively low and the slip in the normal operating range is quite small, less than 5%. As a result it is difficult to vary the speed of an induction motor connected to a constant frequency and voltage using central DC and AC converters or semiconductor devices. DC machines has a relative ease with which its speed can be changed. It is useful in drive systems and used widely in portable power tools in small sizes.

HEAT EXCHANGER: (meeting with Dr. Shelton)

In Dr. Shelton's opinion, he could see no possible means of using a solid absorbent like zeolite as a heat exchanger for space application. He mentioned as a most likely candidate, the use of a pump and piping system connected to a space radiator. He also mentioned that the heat sink to space is -80(deg. F.). Dr. Gene Colwell was mentioned as the expert on this subject. At this time he is supposed to be working on a space radiator for NASA. A fundamental mockup of this system could be envisioned as a potential inclusion that a rankine power plant using water as a system could be utilized to produce power in the system. The problem of doing that is that heat would have to be expelled at a lower temperature. Thereby, requiring a larger radiator. How much power can be produced must be checked in thermobook under assumption of specific temperature range.

POWER SYSTEMS:

The three principle power system which were looked into are brayton, rankine, and thermionics. Some of the characteristics of these power systems are as follows:

System	Characteristics
Brayton	High efficiency Large radiator
Rankine	Lowest weight for given temp. level Smaller radiator area than brayton cycle Two-phase, liquid metal system
Thermionics	Very high temp. High power density Smallest radiator area of the three system.

To obtain good performance of the boiler and the condenser in a Rankine cycle space-power system, the heat-transfer processes associated with two-phase flow of liquid metals must be understood. To obtain an efficient and reliable power system, stable operation of these two components must be obtained, both by themselves and by their interactions with other parts of the system.

Weight is certainly important and, all other things being equal, the lightest power system would be selected. In applications where there is ample weight capabilities and many power systems to choose from, other characteristics besides weight can prevail.

MARSHALL ALLEN:

Visual inspection of similar equipment-e.g. bucket shape, teeth, locations of pins, ect. Looked into information search in library and introduced to CAD system.

CHIH-YU CHU:

Had a meeting with Roger Leung, PhD candidate student in ME dept., about performing static analysis on the digger arms and bucket and found that we need more information before we can make the actual analysis.

JON COLEMAN:

Researched materials on possible use of an induction motor on the lunar digger. There were some advantages and disadvantages of using the induction motor.

JAE N. LIM:

Researched materials on different power systems especially the Rankine system. And typed this weeks progress report.

PAUL THOMAS:

worked on mount and bracket for digger skidder/interface. Performed several sketches and final drawing.

BERTRAN WHEATLEY:

Had an interview with Dr. Shelton and provided us with few tips and ideas. Also worked on the actuators and heat sources.

ME 4182
LUNAR DIGGER GROUP
PROGRESS REPORT #5
MAY 8, 1987

GROUP MEMBERS: MARSHALL ALLEN
CHIH-YU CHU
JON COLEMAN
JAE N. LIM
PAUL THOMAS
BERTRAN WHEATLY

During the past week, we have come up with a couple of concepts for the kinematic design for the placement of the solar radiator. In one configuration, the solar radiator panel is brought straight outwards from the base of the digger arm. The next scheme swings the panel into a position next to the body of the walker. The feasibility of a stationary or rotational mounting to the base is being evaluated in terms of complexity and need.

We searched for hydraulic fluids for the hydraulic actuating system and found two possibilities. Both fluids are manufactured by the Royal Lubricants company. The two fluids are Royco Micronic 846 and Royco 820x. Both fluids are synthetic and designed for high temperature changes. Their range is from -65°F to 400°F . One of these two Royco fluids may become our final choice.

Because of the lower range of the fluid is -65°F and the temperature on the moon may become -200°F , an electrical resistance dipstick heater will be used to heat up the hydraulic fluid to a suitable range for the fluid. A specific model is being researched in catalogs to see if any can operate in the specified range. A temperature sensor in the oil accumulator will signal the microprocessor unit to turn on/off the dipstick.

After speaking with Dr. Johnson about our digging mechanism, he provided us with two IBM programs designed to analyze bolts in shear. Dr. Johnson believes they were the most applicable for our implement.

ME 4182
LUNAR DIGGER GROUP
PROGRESS REPORT # 6
MAY 15, 1987

GROUP MEMBERS: MARSHALL ALLEN, CHIH-YU CHU, JON COLEMAN,
JAE N. LIM, PAUL THOMAS, BERTRAM WHEATLEY

Each member of our group is researching some background information as follows:

SOLAR RADIATOR:

A mechanism for moving the solar panel from underneath the digger was being considered. The following mechanism is the prominent system being currently investigated. Two slider crank mechanisms located on each end of the panel slightly above the panel's center of gravity will move the panel from underneath the walker. A wire rope attached to the top center of the panel will be attached to a pulley system and counterweight which will relieve part of the load from the slider crank linkages, but will mainly adjust the angle of the panel. A brace will be located on the end of each connecting rod to transfer load to the crank linkage and to hold the bars in place.

FORCE ANALYSIS:

The different angles and positions of the arms and actuators were calculated. Buckling forces on each actuator was calculated from actuator dimensions from last quarter. Preliminary analysis on the dimensions of the three interface connections to the walker was done. An initial diameter of 0.5 inches for each connection was calculated. This analysis assumed a factor of safety of 3, 95% reliability, 2024-t36 aluminum alloy, ground finished, tensile preload of 100 lbs., a fluctuating load of 0 to 1600 lbs., and infinite life. This analysis assumes axial loading of the connections.

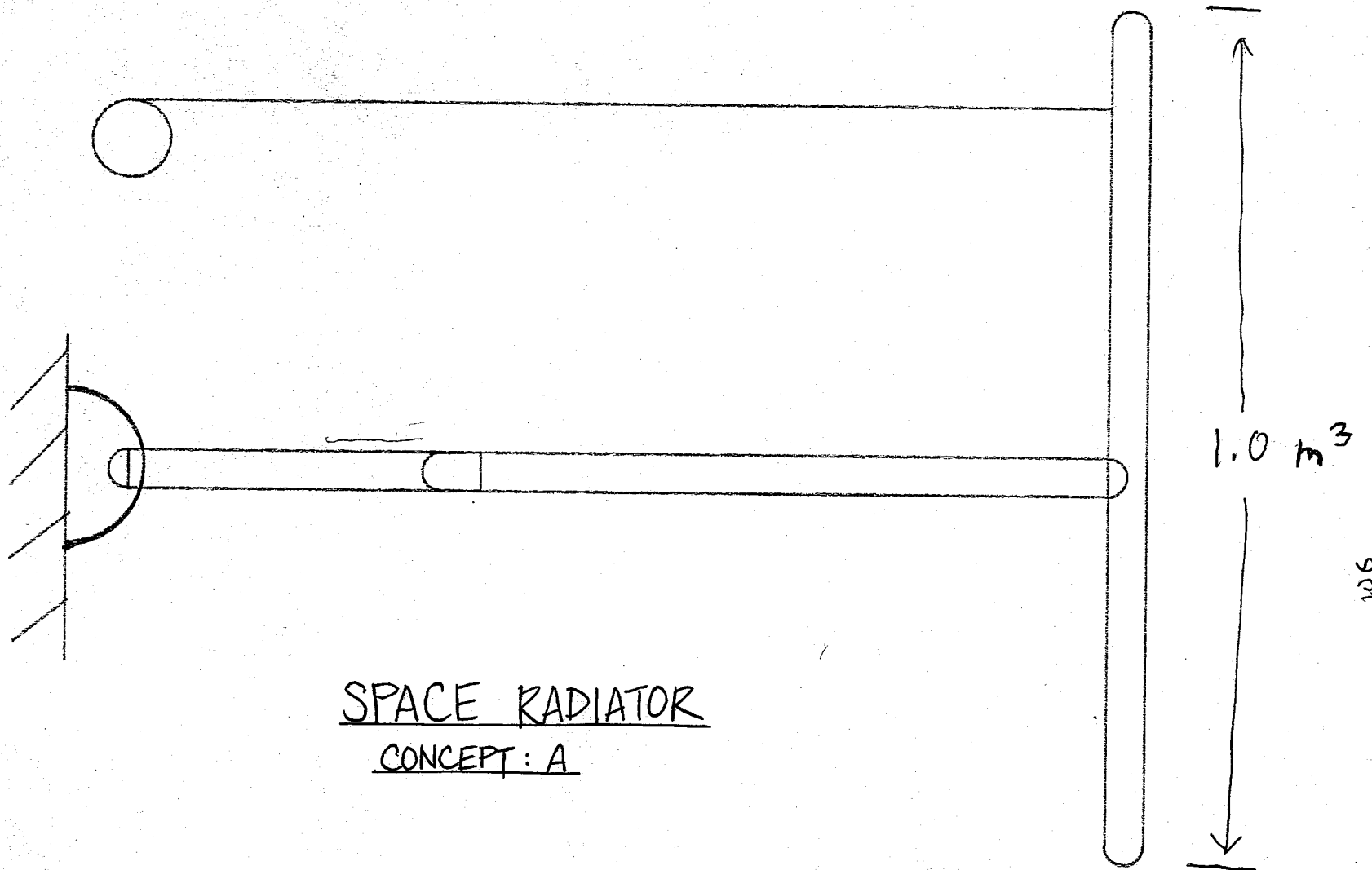
POWER SYSTEMS :

A comparison between hydraulic and electric motors provided the following information :

Hydraulic

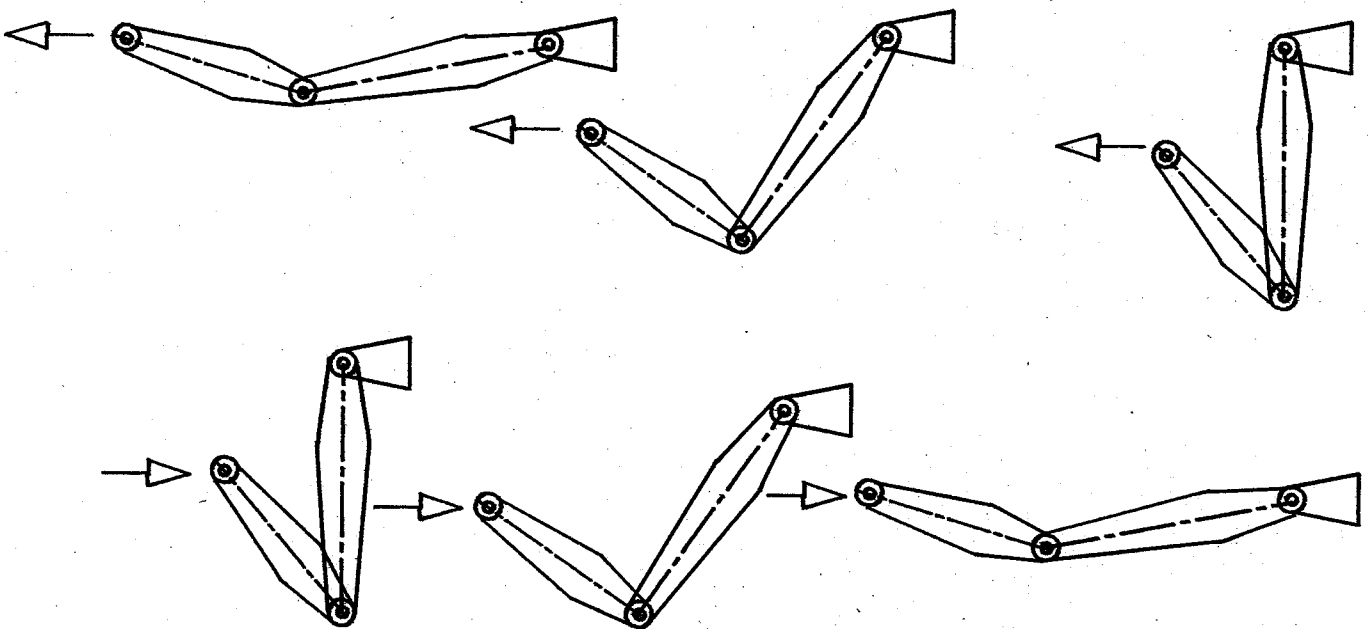
MERITS: High force density; Good controllability ;
Indefinite stall capability; Low actuator inertia;
Simple design; Low actuator cost

DEMERITS: High cost of servovalves; Effect of oil
temperature change on performance; Leakage; Dirt
sensitivity



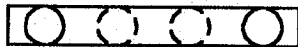
SPACE RADIATOR
CONCEPT: A

PECKING ARRANGEMENT

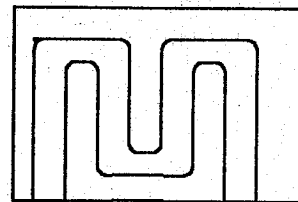


POSSIBLE RADIATORS FOR HEAT TRANSFER

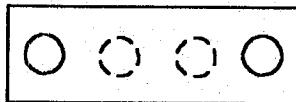
1



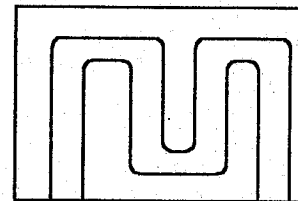
ALUMINUM PIPES WELDED
BETWEEN TWO THIN AL. SHEETS



2

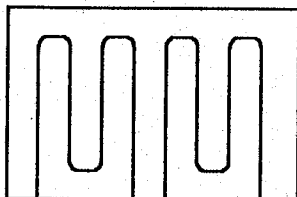


GROOVES DRILLED INTO
ALUMINUM BLOCK



(MOST EFFICIENT RAT MAZE SYSTEM)

3



DIFFERENT SHEETS CAN HOLD DIFFERENT
FLUIDS FOR FLEXIBILITY

ME 4182
LUNAR DIGGER GROUP
PROGRESS REPORT #87
~~APRIL 17~~, 1987

GROUP MEMBERS: JAE LIM
CHIH-YU CHU
PAUL THOMAS
BERTRAM WHEATLY
MARSHALL ALLEN
JON COLEMAN

During this week, we went through the analysis of electric motors, radiation systems, kinematics, power systems, and joints.

ELECTRIC MOTORS

The brushless, Samarium-Cobalt motor designed by General Motors/Delco, used by NASA for Space Shuttle application, has been chosen for our likely motor. Comparisons on the synchronous, induction, and DC motors brought us to the conclusion. One of the best features of the motor include the 89 - 95% efficiency.

HEAT TRANSFER

Radiators were chosen instead of the solid absorbant heat exchanger, since the heat pump process was determined not feasible. The apparatus for mobilizing the radiator has been given two basic ideas. The radiator will either be pushed through the top, or pushed out from the side.

KINEMATICS

Equations for the angles and lengths of the system were made. Various actuators corresponding to the feasible loads was also calculated by the areas and force analysis. Joint and pin force analysis was conducted to find the relative sizes needed.

POWER SYSTEMS

Electromechanical and hydraulics were researched in more depth. Velocities, extension and retracting forces, and horsepower was found. The result of a basic weight to power analysis proved hydraulics better for weight. Damping is yet to be found for the system.

Jae Lim: Research in the electromechanical and hydraulic data including actuators, weights, and efficiencies.

Chih-Yu Chu: Kinematic analysis of the pins and joints. Calculated the maximum force and equations

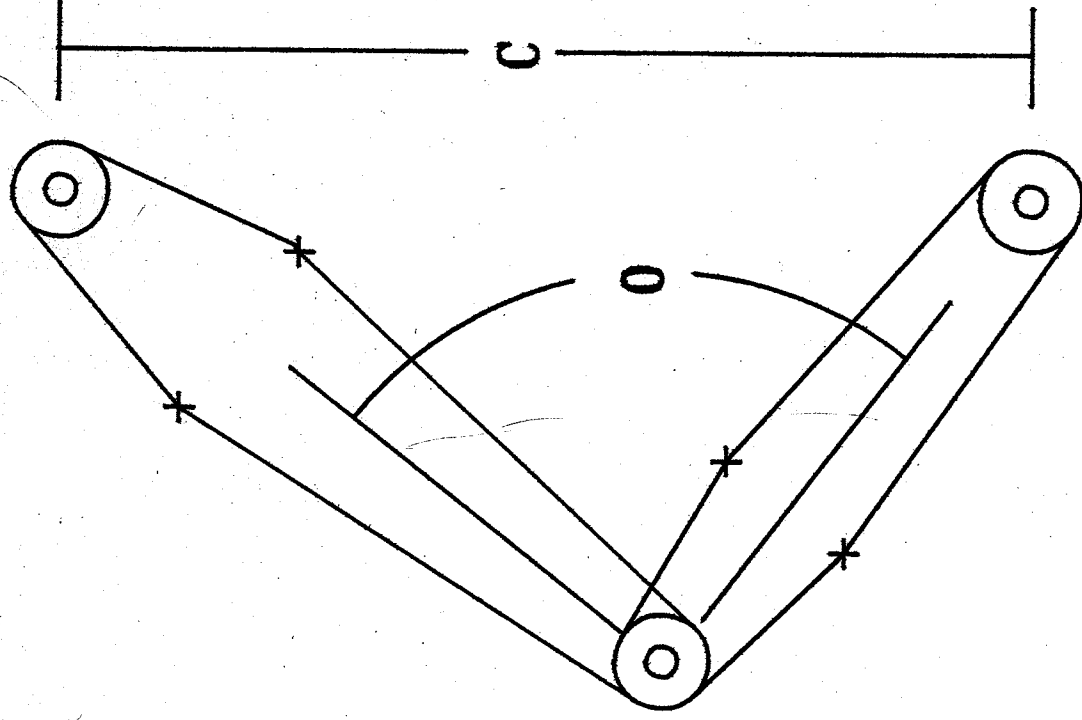
Paul Thomas: DC motor and hydraulic research. End effector design possibilities, fatigue data at cryogenic temperatures, and attempted work on the Geomed.

Bertram Wheatly: Design of the radiation mobilization system side push method as illustrated in the enclosed figure, which he drew.

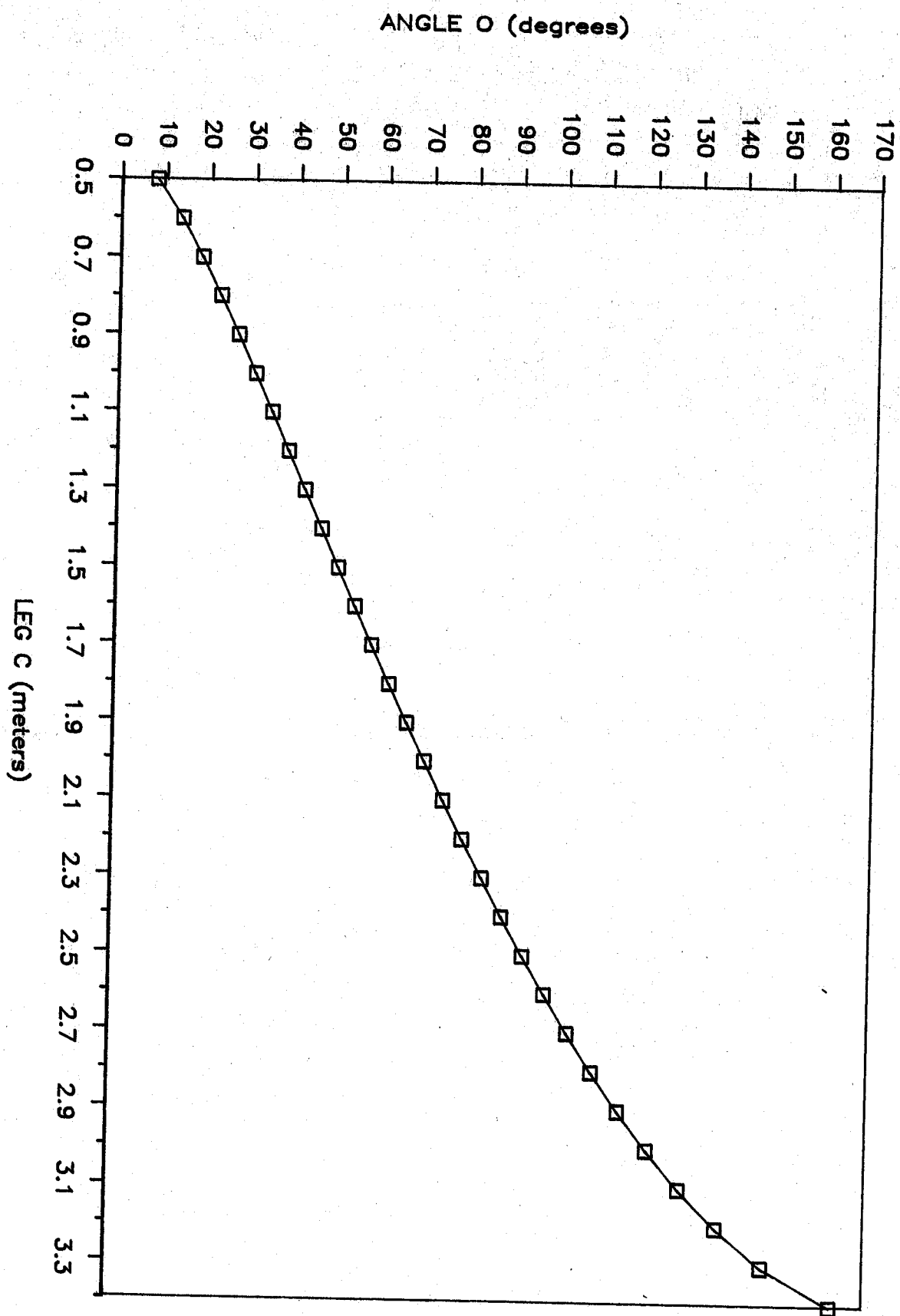
Marshall Allen: Research on the overall structure of the hydraulic system. He also did the computer programing for the forces, angles, and areas.

Jon Coleman: Research on soil mechanics and did some designing of the end effector.

Arm Extension C vs Angle Extension 0



ANGLE O vs. LEG C

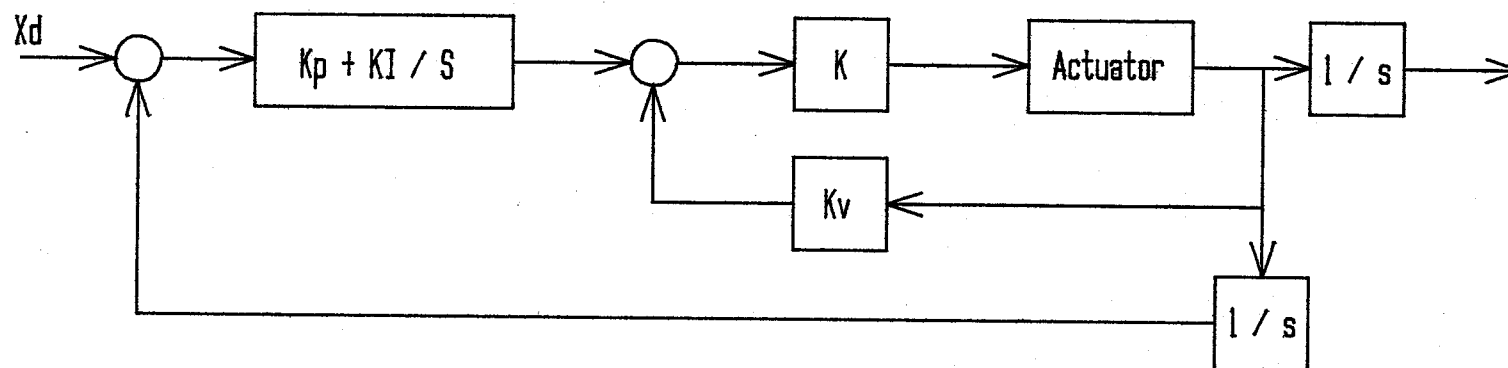


ME 4182
Lunar Digger Group 7
Weekly Progress Report
5-29-87

MARSHALL ALLEN
CHIH-YU CHU
JON COLEMAN
JAE LIM
PAUL THOMAS
BERTRAM WHEATLEY

This week Group 7 met several times to write the rough draft of the final report. Each group member was assigned to write up sections of the report in which he researched earlier during the quarter. Several major sections were covered, including heat transfer, motor selection, the hydraulic system and method of operation. During the next and final week, other sections and subsections will be added with the necessary format for the final report in formal ASME form.

Joint PID Control



This schematic represents the type of control functions necessary at each actuator. The combined information on position and velocity of each actuator will specify the state of the entire digger arm